Macromolecules

pubs.acs.org/Macromolecules Article

# Solvent Properties Influence the Rheology and Pinching Dynamics of Polyelectrolyte Solutions: Thickening the Pot with Glycerol and Cellulose Gum

Leidy Nallely Jimenez, Carina D. V. Martínez Narváez, and Vivek Sharma*

Cite This: *Macromolecules* 2022, 55, 8117–8132 Read Online

ACCESS | Metrics & More | Article Recommendations

**ABSTRACT:** Charge-bearing groups that ionize in solution influence the macromolecular conformations, interactions, and dynamics of polyelectrolytes. The rich and complex shear rheological response of polyelectrolyte solutions and the influence of salt and pH are the focus of many exquisite theoretical and experimental studies. Surprisingly, the influence of solvent properties on the rheological response of polyelectrolyte solutions is not well studied, which motivates this study. Here, we tune the solvent properties by varying the glycerol fraction in glycerol/water mixtures used for dissolving cellulose gum or sodium carboxymethyl cellulose (NaCMC). The rate-dependent steady shear viscosity measured using torsional rheometry shows that cellulose gum and glycerol thicken the pot of aqueous food or pharmaceutical formulations, but the effect is not additive. The thickening behavior is often assessed or tuned in applications and processing by contrasting the delay in pinching of necks formed by dripping or stretching of liquid bridges. As streamwise velocity gradients associated with extensional flows arise in such pinching necks, extensional rheology measurements are needed but are rare due to the longstanding characterization challenges. Here, we utilize dripping-onto-substrate (DoS) rheometry protocols we developed to visualize and analyze the capillarity-driven pinching dynamics and characterize the extensional rheological response. We characterize the influence of NaCMC concentration and glycerol fraction on the shear and extensional rheological response and pinching dynamics of semi-dilute polyelectrolyte solutions. We find that solvent choice and properties offer pragmatic options for macromolecular engineering of formulations in the food, pharmaceutical, and personal care industries that rely on polyelectrolytes as additives and thickeners.

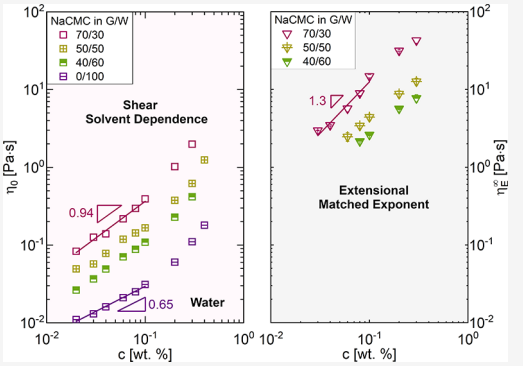




## INTRODUCTION

Biologically sourced polysaccharides and cellulose derivatives are in increasing demand as rheology and processability modifiers for creating sustainable, water-based formulations with minimal or no VOCs (volatile organic compounds) and reduced carbon footprint and pollution.[1−3] The consumer, environmental, and market-driven impetus to increase the use of polysaccharides due to their non-toxicity, biocompatibility, and biodegradability has driven extensive shear rheological characterization of the influence of polymer type, molecular weight ($M_w$), concentration ($c$), polydispersity ($Đ$), degree of substitution (DS), and branching.[1−4] Polysaccharides, such as cellulose gum and xanthan gum, that contain ionizable groups behave as polyelectrolytes,[5−9] acquiring an expanded conformation in solution due to the electrostatic interaction among dissociated ionic groups surrounded by a cloud of counterions along the polymer backbone. Consequently, a significant enhancement in solution shear viscosity, $\eta$, occurs at a relatively low concentration of polyelectrolytes compared with neutral polymers.[5−17] Theoretical and experimental studies show that dynamics, shear rheological response, and processability are influenced significantly by variation in polyelectrolyte concentration, charge fraction, added salt, and pH.[5−28] However, surprisingly, little effort is dedicated to the influence of solvent properties on the rheology of charged polysaccharide (and polyelectrolyte) solutions, primarily motivating this study.

Pressure-driven flows through channels and drag flows near moving surfaces in spreading or coating operations require optimization of shear rheological response as such processes generate shear flows involving velocity gradients perpendicular to the flow direction. Streamwise velocity gradients associated with extensional flows spontaneously arise in converging or diverging channel flows and in capillarity-driven pinching of fluid necks during drop formation and dispensing processes.

Received: January 23, 2022
Revised: August 3, 2022
Published: September 13, 2022





https://doi.org/10.1021/acs.macromol.2c00170
*Macromolecules* 2022, 55, 8117−8132

However, characterization and understanding of shear rheological response often give little or no indication of extensional rheological response and heuristic properties such as jettability, sprayability, stringiness, spinnability, stickiness, gloppiness or gloopiness, ropiness, and coating behavior associated with processability and applications. High sensitivity to deformation history, flow instabilities, need for bespoke instrumentation, and limited range of accessible strain or strain rates pose well-documented challenges for extensional rheology measurements.[29−37] The characterization and analysis of extensional rheology of polysaccharide dispersions with low viscosity and weak elasticity (unmeasurable on standard torsional shear rheometers) remain particularly challenging.[38−40] Early attempts (∼1970−2000) to measure the extensional rheology of polysaccharides, especially xanthan gum, used techniques such as four-roll mill, opposed jets, fiber spinning, orifice flows, and filament stretching rheometer (FISER) that were designed for fluids with shear viscosities greater than 100 times water viscosity.[41−46] Such techniques restrict the measurements of extensional viscosity to relatively low extensional rates (<10 $s^{-1}$).[41−46] The countable few studies of extensional rheology of polyelectrolyte solutions,[42,43,45−61] including the stagnation point flow experiments carried out by the Bristol group[47−49] and by Dunlop and Leal[50,51] in the 1980s, characterized only a few concentrations, often dilute, by using high-viscosity solvents. The concentration dependence remained unexplored for the semi-dilute, unentangled, and entangled polyelectrolyte solutions.

The introduction of methods that analyze capillarity-based pinching, for example, capillary breakup extensional rheometer (CaBER), presented the opportunity to emulate dispensing flows and achieve higher extensional rates ($\dot{\varepsilon}$ > 10 $s^{-1}$).[35,56,62,63] However, due to finite time (∼50 ms) needed for initial step stretch, the characterization of low-viscosity unentangled polymer solutions was beyond the reach of these methods, especially for polysaccharides and polyelectrolytes.[33,35,41,64] In a series of papers, we developed dripping-onto-substrate (DoS) rheology protocols to address many of the characterization challenges, including characterization of extensional rheology of low-viscosity systems such as unentangled solutions of neutral and charged polymers.[18,19,64−70] The DoS rheometry protocols rely on the visualization and analysis of capillarity-driven pinching dynamics of the stretched liquid bridge formed between a nozzle and a sessile drop on a substrate. The extensional relaxation time, $\lambda_E$, and the strain and strain-rate dependent extensional viscosity (also referred to as tensile growth coefficient), $\eta_E = \eta_E^+(t, \dot{\varepsilon})$, are typically extracted from the analysis of radius evolution data.[64−68] The rate-independent steady, terminal extensional viscosity, $\eta_E^\infty$, is also measured occasionally.[64−68] Our previous studies showed that the concentration-dependent variation in the shear and extensional rheological response of aqueous solutions of sodium poly(styrene sulfonate) (NaPSS), poly(acrylic acid) (PAA), and sodium carboxymethyl cellulose (NaCMC) is distinct from the corresponding solutions prepared in a glycerol/water (70/30) mixture.[18,19] To decipher the physicochemical factors that lead to the observed differences on changing the solvent, we contrast the pinching dynamics and shear and extensional rheology of NaCMC solutions prepared in a range of glycerol−water mixtures.

Both glycerol and NaCMC are commonly used as thickeners for increasing the viscosity of formulations. Glycerol has three hydroxyl groups that promote its solubility in water and provide sites for hydrogen bonding. As an additive, glycerol enhances viscosity in multicomponent complex fluids used as food and beverages, pharmaceuticals, cosmetics, and adhesives. Additionally, glycerol is used as a sweetener, plasticizer, lubricant,[71,72] and softener due to its hygroscopic nature that permits moisture retainment[73−77] and prolongs the shelf life of edible films.[78] Besides influencing the viscosity, changing the glycerol fraction in aqueous solutions affects the dielectric constant, refractive index, solvent quality or solvent−polymer interactions (and the Flory−Huggins parameter, $\chi_{FH}$), density, and surface tension. Cellulose gum (NaCMC) is widely used as an additive or a rheology modifier (as a thickener) in consumer products, including food,[79] pharmaceuticals,[80,81] paper, cosmetics, and batteries.[82] The shear rheological response of aqueous NaCMC solutions, with and without salt, is relatively well characterized.[5−7,19,25−28,83−97] In a recent publication,[19] we characterized the role of cellulose gum of $M_w$ = 250 kg/mol or $M_w$ = 250 kDa as a shear and extensional rheology modifier in both the presence and absence of salt. We also discussed the role of cellulose gum as a food thickener, and how many culinary flows encountered during production, consumption, processing, and even aesthetic evaluation and savoring of food involve extensional flow fields.[19] Here, we chose NaCMC with a higher $M_w$ = 700 kg/mol = 700 kDa to characterize the influence of solvent properties on shear and extensional rheological response using solutions formulated in glycerol/water (G/W) mixtures. We picked NaCMC samples with product specification and supplier matched with Lopez *et al.*[5−7,95,98,] and our shear viscosity values match their data. We expect that our extensional rheology datasets provide an essential missing piece of the puzzle for developing constitutive models and a deeper understanding of polyelectrolyte physics. Lastly, we anticipate that the findings would motivate additional studies on the influence of solvent choice on the conformation, dynamics, and rheology of polyelectrolytes and facilitate macromolecular engineering of formulations in the food, pharmaceutical, and personal care industries.

## EXPERIMENTAL METHODS AND MATERIALS

**NaCMC Solutions.** NaCMC of $M_w$ = 250 kDa and $M_w$ = 700 kDa was purchased from Sigma-Aldrich with the DS specified by the manufacturer to be DS= 1.15−1.35 and DS = 0.8−0.95, respectively, and was used without further purification. We picked the NaCMC samples with product specification and supplier matched with Lopez *et al.*[5−7,95,98] to benefit from their shear rheology and scattering studies and careful literature review and comparisons. Lopez *et al.*[5−7,95,98] reported that the measured average molecular weights are $M_w$ = 320 kDa and $M_w$ = 1200 kDa, respectively, in contrast with the as-received $M_w$ = 250 kDa and $M_w$ = 700 kDa values, respectively, and DS = 1.15 for the $M_w$ = 250 kDa. Behra *et al.*[28] determined DS = 0.95 for $M_w$ = 700 kDa and, in agreement with Lopez *et al.*[6], measured a much larger $M_w$ = 1200 kDa. Here, we focus on changes in rheological response due to the variation in glycerol fraction in a solvent comprising glycerol/water (G/W) mixtures. We added the dry NaCMC powder to deionized water first and left the aqueous dispersions on a roller for a minimum of 3 days. After glycerol addition, the solution was left on the roller for a few additional days to ensure a homogeneous dispersion. Milder mixing conditions prevent chain breakup associated with high deformation rate flows.

**Shear Rheological Characterization.** The steady shear viscosity, $\eta(\dot{\gamma}) \equiv \tau_{12}/\dot{\gamma}$, of NaCMC in glycerol/water mixtures was characterized using a concentric cylinder (double gap) Couette cell


https://doi.org/10.1021/acs.macromol.2c00170
Macromolecules 2022, 55, 8117−8132

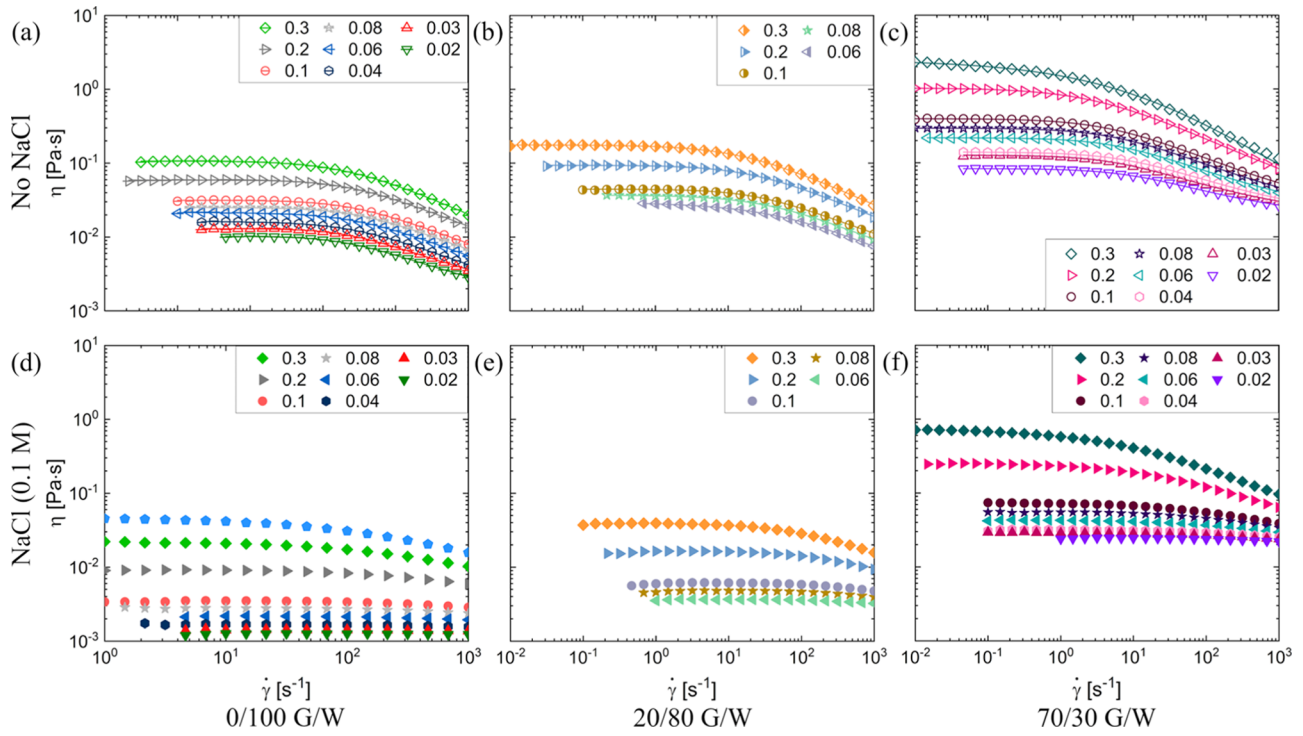


**Figure 1.** Steady shear viscosity of NaCMC solutions prepared in different glycerol/water mixtures (G/W = 0/100, 20/80, and 70/30 w/w). (a–c) Steady shear viscosity as a function of shear rate shows an increase in the extent of shear thinning as glycerol fraction increases. Lines show the Carreau–Yasuda fits made using eq 1. (d–f) Steady shear viscosity curves for the same concentrations as in (a–c) but with salt added (0.1 M NaCl) shows that solution viscosity decreases in all G/W solutions on salt addition.

and cone-and-plate geometry (50 mm diameter, 1° cone angle) on an Anton Paar MCR 302 Rheometer (torque range $10^{-5}$–200 mN m). In response to imposed shear rates, $\dot{\gamma}$, in the range of $10^{-2}$–$10^{3}$ $s^{-1}$, the shear stress, $\tau_{12}$, was measured at a constant temperature (maintained at 25 °C using a Peltier element).

**Extensional Rheological Characterization Using DoS Rheometry.** The extensional rheological response and pinching dynamics were characterized using DoS rheometry for NaCMC solutions formulated in G/W mixtures. The DoS rheometry setup includes a dispensing system for creating a liquid bridge with a neck that undergoes capillarity-driven pinching and an imaging system for visualizing the shape and size of the pinching neck. The dispensing system includes a syringe pump connected to a nozzle (inner and outer diameters, $D_i$ = 0.838 mm and $D_0 = 2R_0$ = 1.27 mm) to deposit a finite volume of sample on a partially wetting substrate at the desired flow rate, Q = 0.02 mL/min, at a height $H$ below the nozzle. The aspect ratio is $H/D \approx 3$. A liquid bridge forms between the nozzle and the substrate. The imaging system consists of a light source, a diffuser, and a Photron Fastcam SA3 high-speed camera with a Nikkor 3.1X zoom lens (18–50) plus a macro lens. The videos, taken at 8000–19,000 fps, are analyzed using ImageJ and specially written MATLAB codes that use edge detection to analyze the capillary thinning and obtain radius evolution data. The outer nozzle diameter is used for determining the pixels per unit length. Pendant drop tensiometry is used to verify that the solvent properties set the surface tension of these polyelectrolyte solutions.

Additional details about the experimental setup and design considerations, specific advantages of DoS rheometry contrasted to other extensional rheology methods, and the various approaches to analyzing radius evolution datasets are included in our previous contributions.[18,19,37,64−70,99−105] We investigate and describe the extensional rheological response of complex fluids such as neutral and charged polymer solutions, inks, nail lacquers, surfactant-based cosmetics (shampoos and conditioners), proteins such as egg albumin, spinnable polymer solutions,[102,105] and foods (honey, molasses, mayo, and ketchup).[18,19,37,64−70,99−105] Since we introduced DoS rheometry in 2015, it has emerged as the method of choice for innumerable studies benefitting from the virtues of a simplified, cost-efficient setup and the ability to analyze the pinching dynamics and extensional rheological response of complex fluids, including those with viscosity comparable to water or weak elasticity, even with sub-millisecond relaxation times.[106−117]

## RESULTS AND DISCUSSION

**Shear Rheology of NaCMC in Glycerol/Water Mixtures.** The steady shear viscosity data plotted for a range of NaCMC concentrations for three different glycerol/water (G/W) systems (0/100, 20/80, and 70/30 w/w) are shown in Figure 1a–c. The corresponding data for salt-added (0.1 M NaCl) solutions are included in Figure 1d–f. For a fixed salt concentration or solvent type, the solution viscosity progressively increases with polyelectrolyte concentration, as observed in each plot. As the relative amount of glycerol in the solvent mixture increases (in each row, left to right), the overall solution viscosity increases, but quantitative analysis shows that the increase is much less than anticipated based on the solvent viscosity increase alone. The dataset in each column contrasts the shear rheological response of the no-salt case with high salt solutions for a range of polyelectrolyte concentrations. The rate-dependent steady shear viscosity data for the no-salt solutions show a well-defined onset of shear thinning for many solutions that exhibit shear rate-independent viscosity on salt addition.

The rate-dependent viscosity can be fit as shown in Figure 1 (for the no-salt-added data) using the Carreau–Yasuda model, given by the following equation

$$\eta(\dot{\gamma}) = \eta_0 + (\eta_0 - \eta_\infty)[1 + (\dot{\gamma}/\dot{\gamma}_c)^a]^{m-1/a} \quad (1)$$


https://doi.org/10.1021/acs.macromol.2c00170
Macromolecules 2022, 55, 8117−8132

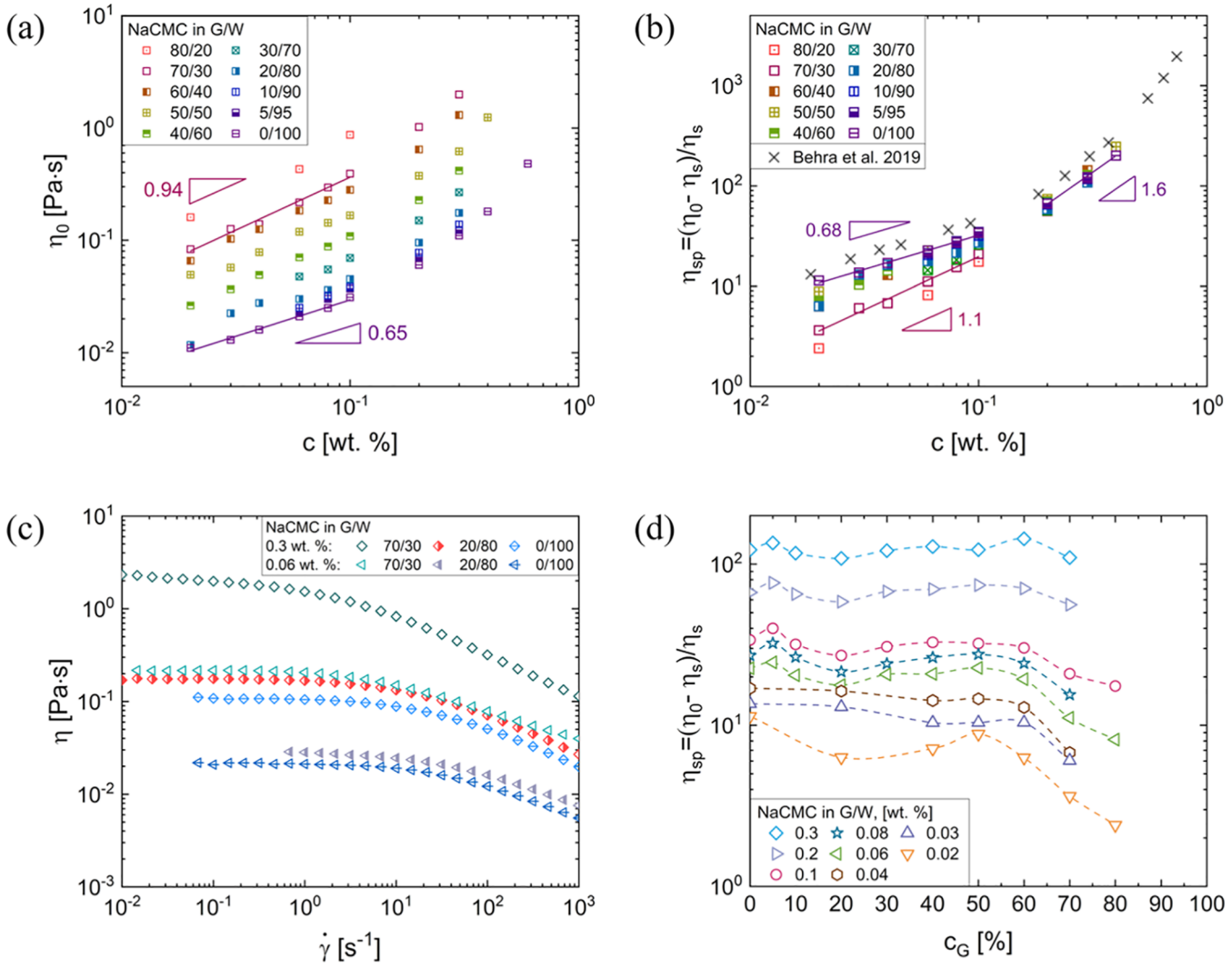


**Figure 2.** Steady shear rheological response for NaCMC in different G/W solutions. (a) Zero shear viscosity as a function of polymer concentration for different G/W mixtures (0/100−80/20 w/w) shows a stronger concentration dependence at higher G/W ratios. (b) Specific viscosity as a function of polymer concentration in different G/W mixtures highlights how the addition of glycerol leads to a progressive decrease in the coil size and stronger concentration-dependent scaling. The data from Behra *et al.*[28] is included to show that identical NaCMC samples are used in both studies. (c) Steady shear viscosity as a function of shear rate measured for 0.06 and 0.3 wt. % NaCMC in solvents with variation in glycerol fraction (0/100, 20/80, and 70/30 w/w). (d) Specific viscosity as a function of glycerol fraction is shown for eight different polymer concentrations and exhibits a non-monotonic dependence on glycerol content.

The Carreau−Yasuda model has five parameters: (i) a rate-independent zero shear viscosity, $\eta_0$, (ii) an infinite or high shear rate viscosity, $\eta_\infty$, (iii) a critical strain rate $\dot{\gamma}_c$, (iv) a transition control factor $a$, and (v) an exponent, $m$, that captures the power law dependence of the viscosity and shear stress on the shear rate in the intermediate shear rate region. For these NaCMC solutions, we equated the high shear rate viscosity, $\eta_\infty = \eta_s$ (solvent viscosity), and reduced the number of parameters to 4. The solvent viscosity, $\eta_s$, as a function of glycerol fraction in the G/W mixture is tabulated in a later section. The magnitude of steady shear viscosity, the degree of shear thinning decrease on salt addition, and the influence of added salt are stronger at lower polymer concentrations. The added salt also causes the onset of shear thinning to shift to higher shear rates, as shown in Figure 1d−f.

Increasing glycerol fraction leads to a proportional increase in the zero shear viscosity of NaCMC solutions as can be observed in data shown in Figure 2a. For a fixed glycerol fraction, the zero shear viscosity displays $\eta_0 \propto c^{0.65}$ for the aqueous solutions and $\eta_0 \propto c^{0.94}$ in the semi-dilute unentangled regime for solutions containing 70% glycerol. A closer look at the zero shear viscosity data shows that the increase observed on glycerol addition is not directly proportional to the increase in solvent viscosity, $\eta_s$. Specific viscosity, $\eta_{sp} = (\eta_0 - \eta_s)/\eta_s$, which scales polymer contribution to solution viscosity with solvent viscosity, as shown in Figure 2b, captures the variations in the polyelectrolyte conformation and intrachain interactions. The overlap concentration, defined here as the concentration at which the solution viscosity is twice the solvent viscosity, is estimated to be $c^*_{0/100} \approx 0.0007$ wt. % for 0/100 G/W and to be $c^*_{70/30} \approx 0.006$ wt. % for 70/30 G/W. The plotted range of NaCMC concentrations lies in the semi-dilute regime as specific viscosity $\eta_{sp} > 1$. The addition of glycerol causes a change in the conformational state of chains, leading to a decrease in the degree of overlap at matched concentration and a reduction in the intrinsic viscosity values calculated using


https://doi.org/10.1021/acs.macromol.2c00170
Macromolecules 2022, 55, 8117−8132

$c^*[\eta] = 1$ from $[\eta]_{0/100} = 1429$ dL/g to $[\eta]_{70/30} = 167$ dL/g. A reduction in intrinsic viscosity on glycerol addition implies a decrease in the pervaded volume of the chain. Intrinsic viscosity in neutral polymer solutions is obtained by extrapolating specific viscosity divided by concentration to the limit of zero concentration. However, the method does not apply to salt-free polyelectrolyte solutions as $\eta_{sp}/c$ increases on dilution and $c^*[\eta] = 1$ provides a robust and pragmatic estimate.[6,22,23]

The specific viscosity versus concentration dataset for non-dilute aqueous NaCMC solutions exhibits two distinct exponents of $\eta_{sp} \propto c^{0.68}$ and $\eta_{sp} \propto c^{1.6}$ in Figure 2b. Since we picked the NaCMC samples with product specification and supplier matched with Lopez *et al.*[5−7,95,98] and Behra *et al.*,[28] the shear viscosity values and exponents we measure for aqueous solutions match with their datasets as shown in Figure 2b. The concentrations for polyelectrolyte solutions prepared by Behra *et al.*[28] accounted for 8.4 wt.% moisture content they measured in the as-received NaCMC. In contrast, our measurements reflect the concentration by weight of the as-received NaCMC, leading to a slight shift in the plotted values. Even though we label our polymers with the supplier-reported $M_w$, we expect that the macromolecular parameters such as the number of Kuhn segments, dispersity, charge fraction, and DS are also similar to those reported by Lopez et al. The exponent of 0.68 or $\eta_{sp} \propto c^{0.68}$ is stronger than $\eta_{sp} \propto c^{1/2}$, associated with the Fuoss law,[118] observed experimentally and anticipated by scaling theories for semi-dilute, unentangled polyelectrolyte solutions.[8,11,14−17,22−24,118−133] Likewise, the exponent of 1.6 or $\eta_{sp} \propto c^{1.6}$ has slightly stronger dependence than 3/2 predicted by Dobrynin, Colby, and Rubinstein[11,15,17,23] and somewhat weaker than 1.7 expected by Muthukumar.[14,127,134] The exponent of 3/2 is reported for entangled solutions of poly(methyl-2-vinyl pyridinium chloride) PMVP-Cl random copolymer in ethylene glycol,[24,135] aqueous NaCMC solutions,[5] and aqueous xanthan gum solutions.[8]

On glycerol addition, the scaling exponent progressively increases in the unentangled semi-dilute regime from $\eta_{sp} \propto c^{1/2}$ for aqueous solutions to $\eta_{sp} \propto c^{1.1}$ for the glycerol−water (70/30) mixture as shown in Figure 2b. However, the exponent of $\eta_{sp} \propto c^{1.6}$ for the second regime appears to be unaffected by the change in glycerol concentration. The physicochemical basis for distinct exponents observed in these two regimes is discussed in the next section. The influence of glycerol concentration on the steady shear viscosity of two NaCMC concentrations, 0.06 and 0.3 wt. %, is shown in Figure 2c (0/100, 20/80, and 70/30). The lower concentration solutions ($c$ = 0.06 wt. %) lie in the unentangled semi-dilute regime and show higher sensitivity to glycerol concentration than the data for $c$ = 0.3 wt. %, which lie in the entangled regime. Figure 2d shows that specific viscosity as a function of glycerol concentration for a range of polymer concentrations ($c$ = 0.02−0.3 wt. %) exhibits a non-monotonic dependence on glycerol concentration, and the strongest influence is manifested at the lowest NaCMC concentrations shown. A similar non-monotonic dependence has also been reported for the specific viscosity of neutral polymers on changing the water fraction in a binary mixed solvent.[102,136] The variation in specific viscosity arises from the combined influence of change in relative coil size and interchain interactions, possibly revealing the interplay of changes in electrostatic interactions, hydrogen bonding, solvent structure, and hydrophobic interactions.

**Crossover Concentration and Role of Electrostatic Interactions.** Scaling theories describe the shear relaxation dynamics of both charged and uncharged polymers in semi-dilute unentangled solutions using the blob model or the composite Rouse−Zimm model.[14,15,17,26,27,66,95,98,137,138] In such models, excluded volume (EV), hydrodynamic interactions (HI), and additional electrostatic interactions in the charged systems are assumed to play a predominant role. Zimm-like dynamics apply at a length scale $r < \xi$ or size smaller than the correlation blob size, and the chain does not feel the presence of other chains. On length scales larger than the blob size, $r > \xi$, the chain effectively behaves like a Gaussian chain of $N/g$ blobs, displaying Rouse-like dynamics due to screened interactions. The relaxation time of the Rouse−Zimm chain $\lambda_{chain} \approx \lambda_\xi (N/g)^2$ incorporates $\lambda_\xi \approx \eta_s \xi^3/kT$ or the timescale associated with the Zimm relaxation within the blob, and the number of monomers in the correlation blob is $g \sim c\xi^3 \sim c^{-1/(3\nu-1)}$. Here, $\nu$ is the solvent quality parameter that captures the extent of polymer chain swelling or collapse due to polymer−solvent interactions. Thus, relaxation time shows the concentration-dependent variation of the form $\lambda \propto c^m$ with the exponent $m = (2 - 3\upsilon)/(3\upsilon - 1)$. For neutral polymers, $m$ = 1/4 for $\upsilon$ = 3/5 (or $m$ = 0.31 for $\upsilon$ = 0.588) for a good solvent and equals $m$ = 1 if EV interactions are screened or absent. For the case of polyelectrolytes, the exponent turns out to be $m$ = −1/2 (if $\upsilon$ = 1 or strong electrostatic-induced stretching is assumed). Therefore, shear relaxation time is expected to increase on dilution in semi-dilute, unentangled polyelectrolyte solutions that are salt-free. On estimating shear modulus as $G \sim cN^{-1}$, and shear viscosity using $\eta \sim G\lambda$, the viscosity of neutral and charged polymers is expected to grow with the exponent $m$ + 1, yielding $\eta_{sp} \propto c^{1/2}$ for charged polymers, which is quite close to 0.68 observed here. Despite the relative success of scaling theory in capturing the exponents for aqueous solutions in salt-free and salt-added solutions, the concentration-dependent variation of specific viscosity of the NaCMC solutions in glycerol−water mixtures cannot be estimated or predicted.

Conventionally, the entanglement concentration, $c_e$, for salt-free polyelectrolyte solutions is defined at the "tripling transition concentration", $c_t$ that captures the regime change from $\eta_{sp} \propto c^{1/2}$ to $\eta_{sp} \propto c^{3/2}$, and the observed exponent of 3/2 is estimated by scaling theories using the following arguments.[8,10,11,14,15,17−19,22−24,135] The longest relaxation time in the entangled regime is estimated using reptation theory by assuming that the dynamics below correlation blob size are Zimm-like, below entanglement length are Rouse-like, and the entanglement length itself is proportional to correlation blob size. Here, modulus is defined using $G \sim \xi^{-3}$ and a concentration-independent variation relaxation time is anticipated for entangled polyelectrolyte chains. We obtain an exponent of 1.6 in this regime from the $\eta_{sp} - c$ plot (Figure 2b) for the aqueous solutions and estimate nearly similar shear relaxation times (concentration-independent) from the onset of shear thinning behavior but only for a limited range of concentrations.

Several recent papers have reexamined the molecular weight-dependent variation of the tripling transition concentration, shear rheology of entangled solutions formed on salt addition, and probed concentration-dependent variation in magnitude and width of plateau modulus for salt-free solutions.[7,25−27,95,98,138] For example, Dobrynin and co-work-


https://doi.org/10.1021/acs.macromol.2c00170
Macromolecules 2022, 55, 8117−8132

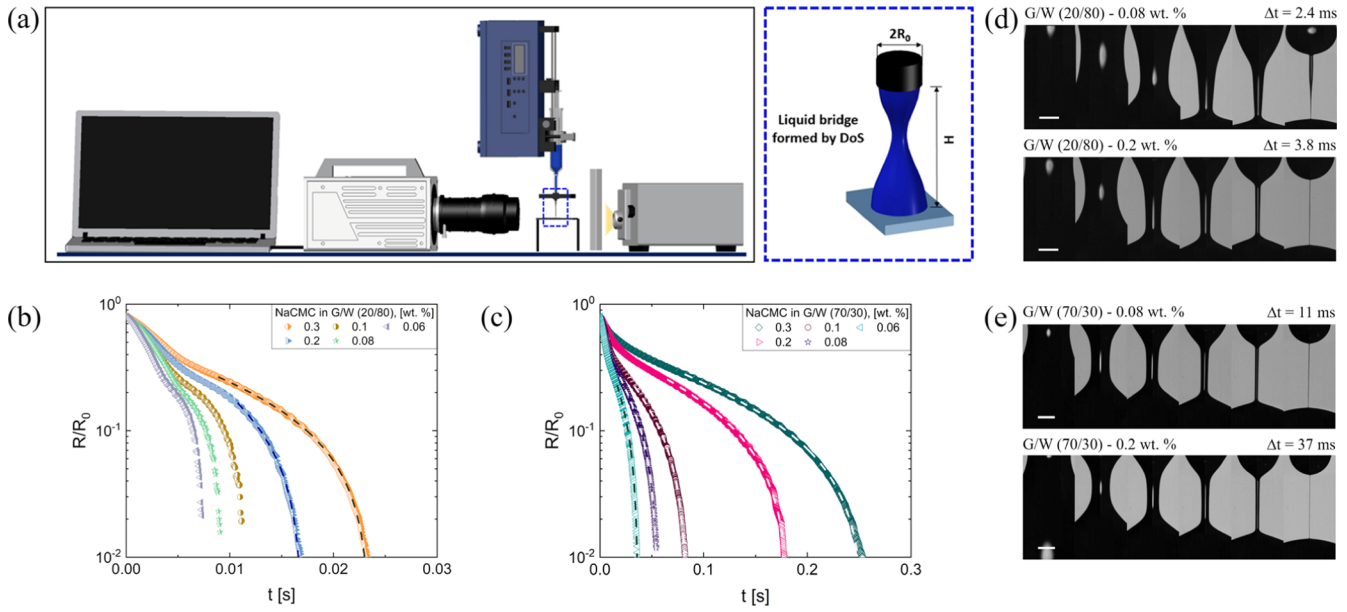


**Figure 3.** Characterization of pinching dynamics and extensional rheology using DoS rheometry. (a) Schematic for DoS rheometry, highlighting the stretched liquid bridge formed between the nozzle and the partial wetting substrate. (b–c) Radius evolution plots for solutions formulated in distinct glycerol fractions (20/80 and 70/30) exhibit a progressively delayed pinch-off as polymer concentration increases. A shorter and distinct first regime is present for solutions formed in a solvent mixture with a higher glycerol fraction. Polymer solutions in low glycerol fraction solvent show a more prominent transition to the viscoelastic response. Dashed lines show the viscoelastic behavior fit using the Anna–McKinley expression (eq 5). (d–f) Image sequences were acquired at 19,000 fps for solutions with 0.08 and 0.2 wt. % NaCMC in low and high glycerol content. The images show qualitatively similar thinning dynamics, except for 0.08 wt. % in 20/80 G/W, which displays a conical-shaped neck connected by a narrow filament to the sessile drop. The scale bar represents 0.5 mm.

ers[25−27] consider the tripling transition from 1/2 to 3/2 to be connected to the overlap of electrostatic blobs and also predict that $\eta_{sp} \propto c^{1/3\upsilon-1}$, implying that the concentration-dependent increase in specific viscosity displays exponents of 1/2, 5/4, or 2, depending on the relative size of the correlation length, electrostatic blob, and thermal blob. Lopez and coauthors,[7,95,98] and also Han and Colby,[138] suggest that the truly entangled behavior is observed well beyond the $\eta \propto c^{3/2}$ regime, which can be termed as a crossover regime between semi-dilute, unentangled, and truly entangled regimes. Assuming that the overall influence of the overlap of electrostatic blobs is to change interactions from the strongly stretched ($\nu = 1$) to weakly expanded chains in a good solvent ($\nu = 0.588$), presents an exponent of 1.31, and allowing some screening such that $0.5 < \nu < 0.588$, pushes the exponent to the values in the range observed in experimental studies of the crossover regime. The NaCMC concentration-dependent variation is found to be independent of solvent properties in this crossover regime, consistent with the idea that EV, HI, as well as electrostatic interactions get progressively screened at higher polymer concentrations.

**Pinching Dynamics of NaCMC Solutions in G/W Mixtures.** The pinching dynamics of NaCMC solutions in different glycerol/water mixtures was characterized using DoS rheometry protocols using the setup shown schematically in Figure 3a. Here, the liquid bridge is created directly from the syringe, so sample volume and any adsorption to the tubing are minimized. Figure 3b,c compares the radius evolution of both semi-dilute unentangled and entangled polymer solutions in low and high G/W ratios, respectively. An increase in glycerol ratio from 20 to 80% provides a pinching time or filament lifespan, $t_f$, that is approximately an order of magnitude higher. As the capillarity-driven instability drives pinching flows, the initial decrease in radius follows an exponential decay captured by linear stability analysis. Subsequently, nonlinear self-similar regimes manifest for both Newtonian and non-Newtonian fluids. The radius evolution data for inviscid fluids, viscous Newtonian fluids, generalized Newtonian fluids (that display shear thinning), and complex fluids (before viscoelastic stresses manifest) can be captured by the following power law expression that incorporates an extensional power law exponent, $n_e$

$$\frac{R(t)}{R_0} = X_x\left(\frac{t_f - t}{t_x}\right)^{n_e} \tag{2}$$

The exponent takes the value of $n_e = 2/3$ for inertiocapillary (IC), $n_e = 1$ for the viscocapillary (VC) pinching, and possibly $n_e = n$ for the power law exponent for the shear thinning fluids. Here, the characteristic time scales for IC and VC behavior is, respectively, called the Rayleigh time, $t_R = (\rho R_0^3/\sigma)^{1/2}$, and viscocapillary time, $t_{vc} = \eta R_0/\sigma$.[34,64,139] The extrinsic length scale, $R_0$, is chosen to be the outer nozzle radius and the parameters viscosity, $\eta$, density, $\rho$, and surface tension, $\sigma$, depending on the fluid choice. The IC regime is observed if the dimensionless measure of viscosity called the Ohnesorge number, $Oh = \eta/\sqrt{\rho\sigma R_0}$, is relatively small or $Oh < 1$, whereas the VC regime arises for $Oh > 1$. The pre-factors $X_x = X_{ic}$ and $X_x = X_{vc}$ for IC and VC regimes, respectively are O(1). Still, mounting evidence,[140−142] including the recent exhaustive reanalysis and review of datasets for Newtonian fluids by Fardin *et al.*,[139] indicates that the pre-factor $X_x$ values for IC or VC need not converge to a single numerical value. Among the solvents, for the low glycerol ratio (<75% by wt.), the pinching dynamics exhibit IC response, whereas for higher glycerol fractions, as $Oh > 1$, VC response is displayed.[34,140,141]


https://doi.org/10.1021/acs.macromol.2c00170
Macromolecules 2022, 55, 8117−8132

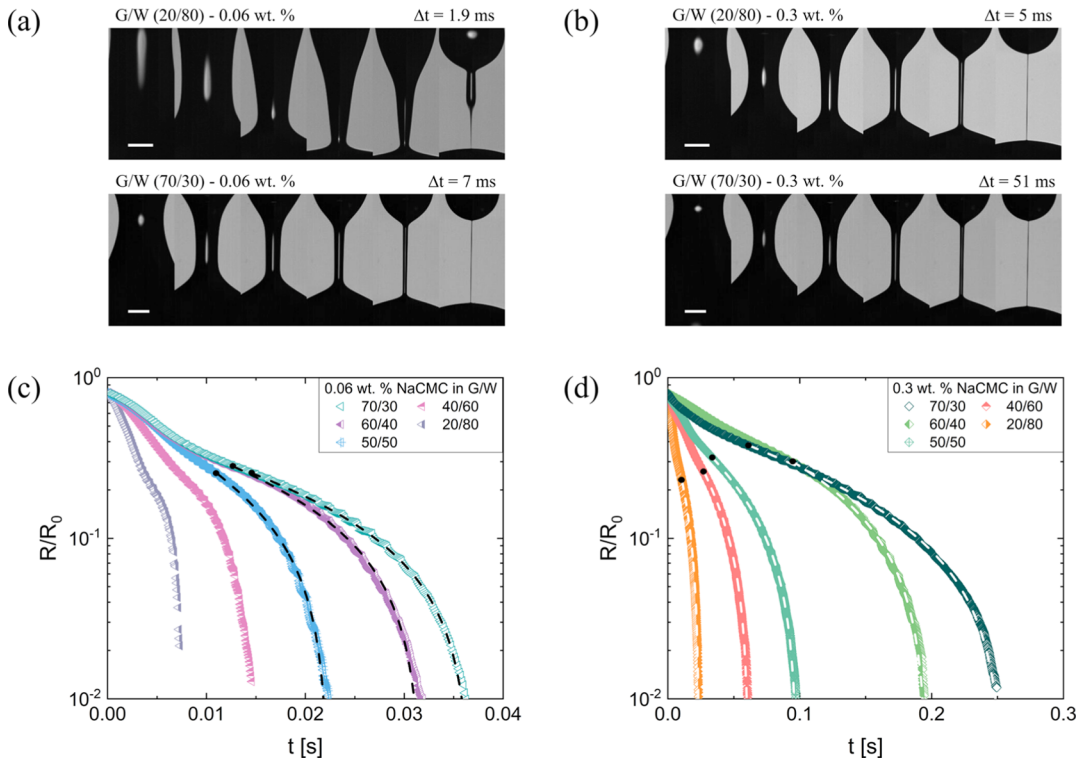


**Figure 4.** Pinching dynamics of NaCMC solutions in glycerol/water mixtures. (a) A conical shape characteristic feature of the inertiocapillary (IC) pinching initially appears for the 0.06 wt. % NaCMC solution in 20/80 G/W represents a lower viscosity case. A slender, cylindrical thread emerges in the late stage due to viscoelastic stresses and delays pinch-off. In contrast, a well-defined slender filament forms for the solution formulated in a higher viscosity solvent (70/30 G/W) from an early stage. (b) Image sequence for 0.3 wt. % NaCMC in 20/80 and 70/30 G/W exhibit slender, cylindrical threads even in the early stage. The scale bars for all cases represent 0.5 mm. (c) Neck radius evolution data, presented on a semi-log scale, show the influence of glycerol fraction on pinching dynamics for unentangled solution (0.06 wt. % NaCMC). (d) Radius evolution data for NaCMC (0.3 wt. %) solutions in the crossover regime (beyond the tripling transition, $c_t$). The dashed lines in (c,d) show the fits obtained using the Anna−McKinley expression used for characterizing the viscoelastic response (see eq 5).

Despite the difference in the early-stage dynamics between Figure 3b,c for the NaCMC solutions formulated with different glycerol fractions, the intermediate regime displays an elastocapillary (EC) response for all solutions. The EC regime results from an interplay of capillarity and nonlinear viscoelastic stresses that arise in response to extensional flows within the pinching necks. The simplest EC expression by Entov and co-workers[62,143−150] uses the shear modulus, $G$, and shear relaxation time, $\lambda$, as parameters. It lacks due consideration of additional effects, including non-Hookean elastic response, finite extensibility, and conformation-dependent drag that arise in response to strong flows for both unentangled and entangled solutions.[34,64−66,69,151−158] Therefore, we use the following modified expression (introduced by Dinic and Sharma[65])

$$\frac{R(t)}{R_0} = \left(\frac{G_E R_0}{2\sigma}\right)^{1/3} \exp\left(-\frac{t - t_c}{3\lambda_E}\right) \tag{3}$$

as it accounts for the onset of EC at $t_c$ and computes an apparent extensional modulus, $G_E$, distinct from the corresponding shear values.[65−69]

Due to finite extensibility effects, a terminal viscoelastocapillary (TVEC) regime manifests close to pinch-off, providing a measurement of a strain and strain rate-independent steady, terminal extensional viscosity, $\eta_E^\infty$. The pinching neck radius in the TVEC regime can be described using the following expression

$$\frac{R(t)}{R_0} = \frac{\sigma}{2R_0\eta_E^\infty}(t_f - t) = \frac{1/2}{\mathrm{OhTr}^\infty}\left(\frac{t_f - t}{t_R}\right) \tag{4}$$

Here, $\mathrm{Tr}^\infty = \eta_E^\infty/\eta_0$ presents the ratio of two steady-state values obtained in extensional and shear rheology measurements. For the NaCMC systems with short EC and TVEC regimes, the radius evolution can be conveniently fit with the following semi-empirical expression proposed by Anna and McKinley[63]

$$\frac{R(t)}{R_0} = A\exp(-B(t - t_c)) - C(t - t_c) + D \tag{5}$$

The parameter $B$ can yield a measure of the longest extensional relaxation time, $\lambda_E$ (= $1/3B$), $C$ provides a measurement of the steady, terminal, extensional viscosity, $\eta_E^\infty$( = $\sigma/2R_0C$), and $D$ can be used to find the filament lifespan ($t_f = t_c + (D/C)$). Figure 3b,c show the Anna−McKinley fits to the radius evolution datasets included here. The image sequences in Figure 3d,e show the typical neck shapes analyzed to obtain radius evolution plots and characterize capillarity-driven pinching dynamics for two polymer solutions prepared with solvent mixtures containing low and high glycerol/water ratios. For 0.08 wt. % in G/W = 20/80, a conical shape connected to a slender cylindrical filament is observed just before the breakup. The conical shape disappears at a higher polymer concentration, and the neck shape before breakup is a cylindrical filament characteristic of


https://doi.org/10.1021/acs.macromol.2c00170
Macromolecules 2022, 55, 8117−8132

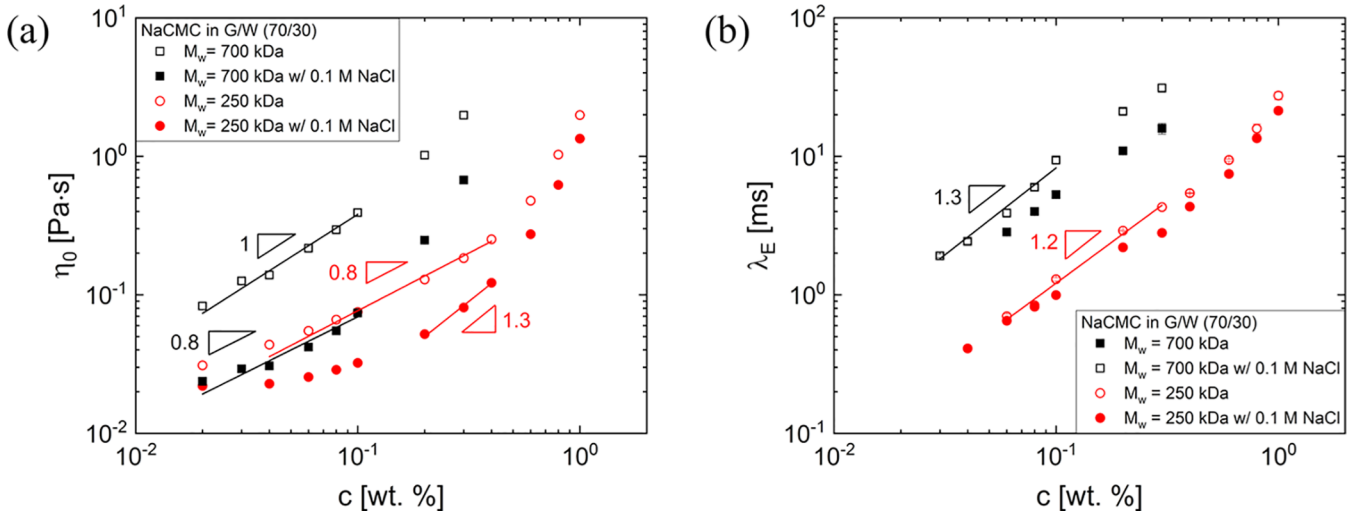


**Figure 5.** Influence of salt and molecular weight on shear and extensional rheological response of cellulose gum solutions. (a) Zero shear viscosity as a function of concentration is compared for NaCMC solutions of two molecular weights ($M_w$ = 250 kDa and $M_w$ = 700 kDa). The data shows that increasing $M_w$ enhances the viscosity. Data shown in closed symbols reveals that just 0.1 M salt leads to a significant reduction in coil dimensions and solution viscosity compared to no salt (open symbols). (b) The extensional relaxation time *vs* concentration data for NaCMC solutions are strongly impacted by the $M_w$ change but exhibit similar concentration-dependent variation in the semi-dilute unentangled regime in low-salt (open symbols) and high-salt (closed symbols) solutions for fixed $M_w$ and solvent type.

predominant viscoelastic effects. A slender cylindrical filament manifests in a higher glycerol ratio (70/30) for 0.08 and 0.2 wt. %. Such conical shapes are associated with the IC response that arises for inviscid fluids with Oh < 1 (the case here).

Figure 4a,b shows the influence of changing glycerol concentration on the neck shape and shape evolution for one representative example of semi-dilute NaCMC solutions above and below $c_t$. A conical shape that connects the pendant drop to the sessile drop through a narrow slender filament can be observed clearly in Figure 4a for the $c$ = 0.06 wt. % solutions made in 20/80 G/W. The shape is consistent with the IC response anticipated for the relatively low viscosity system, with viscoelastic effects manifested in the last stages before the pinch-off event. As the glycerol fraction and shear viscosity increase, the conical shape evolves into a slender cylindrical thread. Radius evolution data extracted from the neck shape analysis is shown in a semi-log plot in Figure 4c for the unentangled solutions ($c^* < c < c_t$) and Figure 4d for the solutions in the crossover regime ($c > c_t$). The addition of glycerol causes an increase in filament lifespan or breakup time. Likewise, a 10-fold increase in filament lifespan is observed in Figure 4d for a 5-fold increment in polyelectrolyte concentration concerning the datasets shown in Figure 4c presented for 0.06 wt. % NaCMC.

The radius evolution data for the NaCMC solutions with $M_w$ = 700 kDa are reminiscent of the datasets presented in our earlier studies for solutions of NaCMC of a lower $M_w$ = 250 kDa as well as of NaPSS solutions and polysaccharide solutions (including hydroxyethyl cellulose or HEC) in having a relatively short apparent viscoelastic response.[18,19,37,69] In contrast, the radius evolution data for highly flexible and highly extensible polymers such as poly(ethylene oxide) show a sharp transition from initial Newtonian-like response to the elastocapillary regime, providing a substantial contribution to filament lifespan.

Figure 5 compares zero shear viscosity and extensional relaxation time for two molecular weights of NaCMC ($M_w$ = 250 kDa and $M_w$ = 700 kDa). The addition of salt leads to a significant decrease in zero shear viscosity and increases the overlap concentration. For example, the solutions made with a lower $M_w$ = 250 kDa display a semi-dilute regime for low salt solutions even for $c$ < 0.1 wt. % due to electrostatic-induced stretching. However, in the high salt limit, several solutions at matched NaCMC concentrations show shear rheological response corresponding to the dilute regime, as the addition of salt reduces the electrostatics-induced stretching. In striking contrast, however, the extensional rheological data for no-salt and high-salt systems show similar concentration dependence for both molecular weights. As the extensional rheological response is dictated by the hydrodynamics of stretched chains only, rather than conformations and interactions of mildly perturbed coils, neither the influence of salt nor of solvent is manifested as strongly as for shear rheological data. The concentration-dependent increase in extensional relaxation time shows the same exponent in both regimes for these NaCMC solutions. According to the blob model, the addition of salt progressively transforms the shear relaxation dynamics, from the polyelectrolyte to neutral polymer values,[6] and the shear rheological response here shows the anticipated sensitivity to salt concentration.

**Extensional Viscosity of NaCMC Solutions in G/W Mixtures.** The strain and strain rate-dependent extensional viscosity (or tensile growth coefficient), $\eta_E = \eta_E^+(t, \dot{\epsilon})$, of NaCMC solutions prepared in G/W (70/30) mixture shown in Figure 6 is determined from the ratio of the capillary stress $\sigma/R(t)$ to the extensional rate, $\dot{\epsilon}(t) = -\frac{2\dot{R}(t)}{R}$, by using the following equation

$$\eta_E = \frac{\sigma}{R(t)\dot{\epsilon}(t)} = \frac{\sigma}{-2\dot{R}(t)} \quad (6)$$

Although the extensional rate remains constant during the elastocapillary regime, with a value $\dot{\epsilon}_{EC}(t) = 2/3\lambda_E$ set by the extensional relaxation time, in the TVEC regime $\dot{\epsilon}(t) = 2(t_f - t)^{-1}$, the deformation rate rises significantly as the pinch-off event is approached. The extensional rates


https://doi.org/10.1021/acs.macromol.2c00170
Macromolecules 2022, 55, 8117−8132

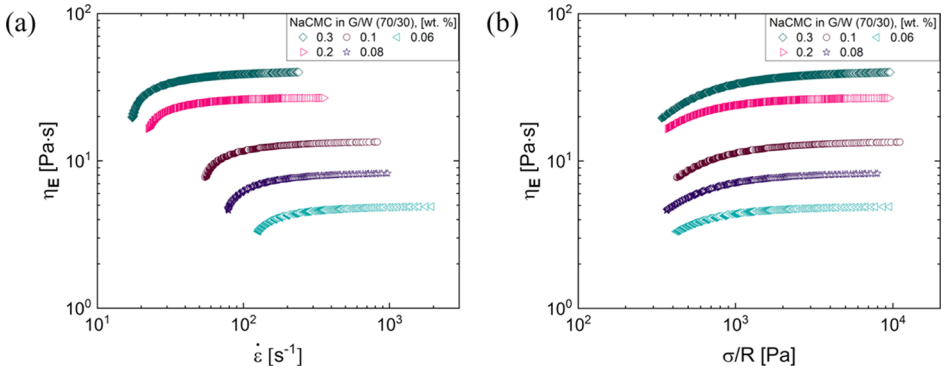


**Figure 6.** Comparison of extensional viscosity as a function of extension rate and capillary stress. (a) Extensional viscosity values measured for NaCMC solutions in G/W (70/30) mixtures plotted as a function of extension rates reveal the extent of strain hardening and the extensional viscosity (and Trouton ratio) and relative increase with NaCMC concentration. (b) The extensional viscosity values shown in (a) are replotted here as a function of capillary stress. The maximum stress is set here by the limit of optical resolution.

inferred from the radius evolution data, shown on the x-axis in Figure 6a, are relatively high (compared to the rates accessible on conventional devices such as FISER) and represent the deformation rates encountered in free-surface flows. These NaCMC solutions show considerable extensional strain-hardening response, even though the shear viscosity exhibits a rate-dependent decrease associated with shear thinning caused by the orientation of mildly perturbed coils. Though the range of extensional rates realized for each solution is different, Figure 6a shows that the rate-independent steady, terminal extensional viscosity, $\eta_E^\infty$, is measured for each concentration.

In Figure 6b, the extensional viscosity is plotted as a function of capillary pressure or the stress that drives the flow. Unlike extensional rate, the stress range is nearly similar for all the solutions, and here, the maximum stress value is set by the optical resolution of the imaging system. In contrast, the minimum is bounded by the radius of the nozzle. We have verified that all datasets show similar stress dependence by rescaling the y-axis with terminal extensional viscosity for each concentration. Like extensional stress (= capillary stress), the Hencky strain or the total accumulated strain in the liquid filament, $\varepsilon = 2\ln(R_0/R(t))$, increases steadily. Hence, conventionally, the apparent extensional viscosity measured using capillarity-based techniques is often plotted as a function of the Hencky strain. The plot of extensional viscosity versus Hencky strain looks quite similar to Figure 6b, though plotting the apparent extensional viscosity as a function of transient extensional stress reemphasizes that the pinching dynamics are driven by variation in capillary stress.

**Extensional Relaxation Time and Steady, Terminal Extensional Viscosity.** The extensional relaxation time, shown in Figure 7a, exhibits a concentration-dependent increase $\lambda_E \propto c^{1.3}$ for the explored concentration range. Despite the change in glycerol fraction, a similar exponent is observed for all solutions. In contrast, the exponents displayed by specific viscosity and zero shear viscosity (in Figure 2) depend on the glycerol fraction, showing that polymer conformations and interchain interactions depend on the solvent properties. The filament lifespan in Figure 7b indicates nearly linear concentration dependence, $t_f \propto c^1$. The absolute value of extensional relaxation time does increase with an increase in the amount of added glycerol. Still, the manifestation of an almost constant scaling exponent highlights that the interactions between hydrodynamically stretched chains in these concentrations are relatively insensitive to changes in electrostatic interactions. A similar but linear concentration dependence was reported for the intrinsically semi-dilute, unentangled PEO solutions by Dinic *et al.*,[66] who argued that the scaling exponent of 1 can be obtained using the Rouse−Zimm chains if the EV interactions are assumed to be screened at all length scales. Figure 7c presents the terminal extensional viscosity obtained from radius evolution fits to the TVEC region ($\eta_E^\infty = \sigma/2R_0C$). All the three quantities obtained from DoS rheometry protocols and shown in Figure 7a−c for NaCMC solutions for different G/W mixtures are included in Table 1.

To explicitly characterize the relative polymer contribution to both extensional and shear viscosity, we define a specific, terminal Trouton ratio $Tr_P^\infty = (\eta_E^\infty - 3\eta_S)/(\eta_0 - \eta_S)$. According to the FENE-P constitutive model, low concentration asymptote of the $Tr_P^\infty$ is a measure of extensibility (the ratio of stretched chain size to the equilibrium coil size). For a fixed glycerol−water ratio, the $Tr_P^\infty$ values shown in Figure 7d appear to be nearly constant $Tr_P^\infty \approx 20-40$ as a function of polymer concentration. In contrast, unentangled solutions of flexible polymers such as PEO (1000 kDa) often display much larger $Tr_P^\infty \approx 10^2-10^4$.

Finally, a close examination of $Tr_P^\infty$ values as a function of glycerol concentration shows nonlinear variation, possibly correlated with the non-monotonic variation of specific viscosity, discussed earlier. However, the data included in Table 1 and Figure 7 show that for cases that show a specific viscosity decrease with glycerol concentration, the specific, terminal Trouton ratio values increase with glycerol concentration, reflecting that chains need to extend more. The analysis of the radius evolution data for aqueous solutions does not reveal an elastocapillary regime for the imaging parameters used in this study. The viscoelastic effects are harder to detect for lower polymer concentration decreases. The lowest polymer concentration for which viscoelastic effects are measurable or manifested in capillarity-based rheometry studies is a function of chain flexibility and extensibility, as was shown recently by Dinic and Sharma.[69] Since NaCMC is semi-flexible and has low extensibility, the qualitative trends emulate the behavior observed for hydroxyethyl cellulose (HEC), with short-lived EC and TVEC regimes.

The change in the shear and extensional rheological response of NaCMC on the addition of glycerol suggests


https://doi.org/10.1021/acs.macromol.2c00170
Macromolecules 2022, 55, 8117−8132

Table 1. Concentration-Dependent Values of Zero Shear Viscosity, Relative Viscosity (Zero Shear Viscosity Scaled with Solvent Viscosity), Shear Relaxation Time and Power Law Index Obtained From the Carreau Model Fit to Steady Shear Viscosity Data and Extensional Relaxation Time, and Steady, Terminal Extensional Viscosity Values Obtained from the Analysis of the Radius Evolution Data Obtained Using DoS Rheometry for NaCMC Solutions in G/W Mixtures[a]

| $c$ [wt. %] | $\eta_0$ [Pa·s] | $\eta_r$ [-] | $\lambda_c$ [s] | $m$ [-] | $\lambda_E$ [ms] | $\eta_E^\infty$ [Pa·s] | Oh |
|---|---|---|---|---|---|---|---|
| Glycerol/Water (0/100) | | | | | | | |
| 0.30 | 0.11 | 124 | 0.042 | 0.55 | | | 0.52 |
| 0.20 | 0.060 | 67 | 0.041 | 0.60 | | | 0.28 |
| 0.10 | 0.032 | 36 | 0.036 | 0.60 | | | 0.15 |
| 0.08 | 0.025 | 28 | 0.030 | 0.59 | | | 0.12 |
| 0.06 | 0.021 | 24 | 0.027 | 0.56 | | | 0.10 |
| 0.04 | 0.016 | 22 | 0.030 | 0.56 | | | 0.08 |
| 0.03 | 0.013 | 15 | 0.047 | 0.61 | | | 0.06 |
| Glycerol/Water (20/80) | | | | | | | |
| 0.30 | 0.18 | 113 | 0.056 | 0.53 | 2.5 | 3.5 | 0.83 |
| 0.20 | 0.095 | 59 | 0.045 | 0.57 | 1.2 | 2.2 | 0.44 |
| 0.10 | 0.045 | 25 | 0.038 | 0.59 | | | 0.21 |
| 0.08 | 0.036 | 23 | 0.023 | 0.53 | | | 0.17 |
| 0.06 | 0.03 | 19 | 0.010 | 0.42 | | | 0.14 |
| Glycerol/Water (70/30) | | | | | | | |
| 0.30 | 2.0 | 112 | 0.06 | 0.22 | 31 | 43 | 2 |
| 0.20 | 1.0 | 56 | 0.28 | 0.52 | 21 | 32 | 1 |
| 0.10 | 0.40 | 22 | 0.19 | 0.55 | 9.4 | 15 | 0.4 |
| 0.08 | 0.30 | 17 | 0.16 | 0.56 | 6.0 | 8.9 | 0.3 |
| 0.06 | 0.22 | 12 | 0.16 | 0.57 | 3.9 | 5.7 | 0.22 |
| 0.04 | 0.14 | 8 | 0.10 | 0.55 | 2.4 | 3.5 | 0.14 |
| 0.03 | 0.13 | 7 | 0.17 | 0.58 | 1.9 | 3.0 | 0.13 |

[a]Ohnesorge number, Oh, is computed using nozzle size as the external length scale.

that all polyelectrolytes could exhibit similar sensitivity to solvent properties. Using datasets included in our two previous studies for PAA, NaPSS, and a lower molecular weight NaCMC, we explore the influence of adding glycerol by contrasting the response in an aqueous solution with solutions made in a 70/30 G/W mixture. Table 2 includes the overlap concentration, intrinsic viscosity, entanglement concentration, and Zimm relaxation time measured or computed for three polyelectrolytes in water and a 70/30 G/W mixture as a solvent. Changing the solvent from water to 70/30 G/W causes a 30-fold increase in solvent viscosity, a decrease in dielectric constant by 68%, and an increase in density by a factor of 1.19. The difference in solvent quality causes changes in polymer−solvent interactions that contribute to conformational changes in the chain and subsequent variation in polymer solution properties.

A comparison of shear viscosity of NaCMC (Table 2) for 0.03 wt. % in G/W (70/30) shows an increase in solution viscosity by 13 times even though the solvent viscosity increases by a factor of 20. For NaCMC with $M_w$ = 700 kDa, the overlap concentration $c^*$, estimated as twice the solvent viscosity, is $c^*_{0/100} \approx 0.0007$ wt. % and $c^*_{70/30} \approx 0.006$ wt. % for 0/100 and 70/30 G/W, respectively. The corresponding intrinsic viscosity values calculated using $c^*[\eta] = 1$ are $[\eta]_{0/100}$ = 1429 dL/g and $[\eta]_{70/30}$ = 167 dL/g. The reduction of the intrinsic viscosity on the addition of glycerol is more than 8-fold, implying that as the G/W ratio increases, a less expanded conformation or a smaller pervaded volume of the chain is obtained. This also leads to a shift in both overlap concentration, $c^*$, and the tripling transition concentration, $c_t$ (which was often presented as entanglement concentration, $c_e$, in the literature).

The Zimm time is higher for the G/W case (for the polyelectrolyte chain in the single-chain limit), and using the formula $\lambda_z = \Lambda[\eta]\eta_s M_w/RT$ gives an estimate of $\lambda_z \approx 17$ ms and $\lambda_z \approx 39$ for water and 70/30 G/W, respectively. However, a decrease in almost 3 times the molecular weight for the same semi-flexible polysaccharide (NaCMC $M_w$ = 250 kDa) only caused a 4-fold decrease of intrinsic viscosity for water with respect to the 70/30 G/W case. A comparable decrease in intrinsic viscosity, 5-fold for NaPSS and 4-fold for PAA, that on changing the solvent from aqueous to 70/30 G/W was reported in a previous contribution.[18] However, a neutral polymer such as PEO in an aqueous solution shows a much smaller intrinsic viscosity and much higher $c^*$ (0.17 wt. % for $M_w$ = 1000 kg/mol) in comparison to all the polyelectrolytes in an aqueous solution, thereby showing that the polyelectrolyte chains have electrostatics induced stretching which gets affected (due to polymer−solvent interactions) on changing the solvent (quality and dielectric constant).

## CONCLUSIONS

In this contribution, we characterized the influence of changing physicochemical properties of the solvent on the dynamics and rheology of polyelectrolytes in semi-dilute solutions. The pinching dynamics and rheological response of solutions of NaCMC ($M_w$ = 700 kDa) in glycerol/water (G/W) mixtures with varied glycerol fraction (0−80% by wt. in solvent mixture) displays a profound influence of solvent choice and composition. NaCMC is a charged polysaccharide that is often referred to as cellulose gum and is widely used as a thickener or rheology modifier in consumer products. Likewise, glycerol is often added to thicken aqueous formulations, especially foods and cosmetics. Though the steady shear viscosity measurements were made for solutions with well-beyond overlap concentration, extrapolation to a specific viscosity of 1 gives estimates of $c^*_{0/100} \approx 0.0007$ wt. % for aqueous solutions and an order of magnitude higher value of $c^*_{70/30} \approx 0.006$ wt. % in G/W (70/30) mixture. The intrinsic viscosity values estimated using $c^*[\eta] = 1$ for NaCMC in water and G/W (70/30) are $[\eta]_{0/100}$ = 1429 and $[\eta]_{70/30}$ = 167, respectively. The decrease in intrinsic viscosity for the higher glycerol concentration indicates a considerable change in polymer−solvent interactions that drives the coil to a more collapsed state. Likewise, even though glycerol addition increases the solvent viscosity, the decrease in pervaded volume causes the specific viscosity that quantifies polymer contribution to viscosity to decrease. Furthermore, the concentration-dependent increase in specific viscosity shows weaker dependence of $\eta_{sp} \propto c^{0.68}$ in semi-dilute aqueous solutions than observed for glycerol-added dispersions with $\eta_{sp} \propto c^{1.1}$ in G/W (70/30) mixtures. A simple estimate of the change in electrostatic interactions due to a decrease in the dielectric constant of the solvent on the addition of glycerol does not explain the dramatic change in size or the exponents that describe concentration dependence.

Specific viscosity versus concentration plots for the non-dilute NaCMC solutions show two distinct regimes. For aqueous NaCMC solutions, the exponents 0.68 and 1.6 that


https://doi.org/10.1021/acs.macromol.2c00170
Macromolecules 2022, 55, 8117−8132

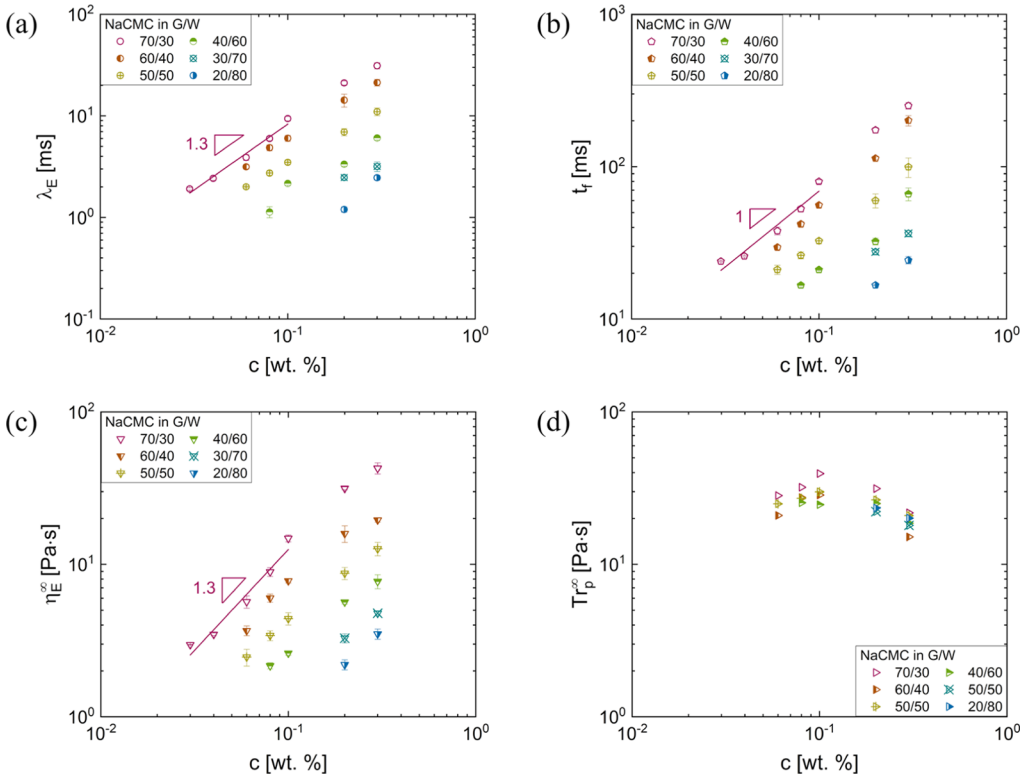


**Figure 7.** Extensional rheological response of NaCMC solutions in G/W mixtures. (a) Extensional relaxation time, $\lambda_E$, as a function of polymer concentration, $c$. (b) Filament lifespan, $t_f$, variation with polymer concentration, $c$. (c) Steady, terminal extensional viscosity, $\eta_E^\infty$, *vs* $c$ data reveal a similar dependence on $c$ as is observed for $\lambda_E$. (d) Terminal Trouton ratio, $Tr_p^\infty$, computed for various NaCMC solutions in a range of glycerol/water mixtures shows nearly similar values, ranging between 20 and 40. Here, the three parameters $\lambda_E$, $t_f$, and $\eta_E^\infty$ were obtained by fitting the Anna−McKinley expression (eq 5) to the radius evolution data acquired using DoS rheometry.

**Table 2. Solvent Viscosity, Molecular Weight, Overlap Concentration, Tripling Transition Concentration, Intrinsic Viscosity, Degree of Overlap at the Tripling Transition Concentration, and Zimm Relaxation Time for NaCMC, NaPSS, and PAA for Aqueous (aq) and G/W (70/30) Systems**

| | NaCMC aq | NaCMC G/W | NaCMC aq | NaCMC G/W | NaPSS aq | NaPSS G/W | PAA aq | PAA G/W |
|---|---|---|---|---|---|---|---|---|
| $\eta_s$ [mPa·s] | 0.89 | 17.9 | 0.89 | 17.9 | 0.89 | 26.8 | 0.89 | 26.8 |
| $M_W$ [kDa] | 250 | 250 | 700 | 700 | 1000 | 1000 | 450 | 450 |
| $c^*$ [wt. %] | 0.007 | 0.03 | 0.0007 | 0.006 | 0.02 | 0.1 | 0.05 | 0.2 |
| $c_t$ [wt. %] | 0.37 | 0.51 | 0.18 | 0.13 | 1 | 1 | 1.5 | 1 |
| $[\eta]$[dL/g] | 143 | 33 | 1429 | 167 | 50 | 10 | 20 | 5 |
| $c_t/c^*$ | 53 | 17 | 257 | 22 | 50 | 10 | 30 | 5 |
| $\lambda_Z$ [ms] | 0.59 | 2.8 | 17 | 39 | 0.82 | 4.9 | 0.15 | 1.3 |

capture the concentration-dependent increase are well matched with the previous studies of aqueous solutions of cellulose gum. The regime change in $\eta_{sp} - c$ plots from $\eta_{sp} \propto c^{1/2}$ to $\eta_{sp} \propto c^{3/2}$ was conventionally described as associated with entanglement concentration, $c_e$, for salt-free polyelectrolyte solutions. However, significant discussion in recent studies defines the $\eta_{sp} \propto c^{3/2}$ regime as a crossover regime that appears before the intrinsically entangled polymer solution behavior is observed, with the exponent for concentration-dependent variation matched with the exponent observed for entangled solutions of uncharged polymers. As a recognition of the importance of the concentration associated with $\eta_{sp} \propto c^{1/2}$ to $\eta_{sp} \propto c^{3/2}$ transition observed for many polyelectrolyte solutions, we christen it as the "tripling transition concentration", $c_t$. On glycerol addition, the exponents for unentangled semi-dilute solutions dramatically change for $c < c_t$ regime. However, beyond the tripling transition concentration, $c_t$ = 0.13 wt. %, solutions with different glycerol content show matched specific viscosity values, implying that all local interactions, including the electrostatic, EV, and HI, are screened out. However, the value of $c_t/c^*$ changes from $c_t/c^*$ = 257 in water down to $c_t/c^*$ = 22, and observed values are significantly higher than $c_t/c^*$ values reported for neutral polysaccharides.

The pinching dynamics and extensional rheological response of NaCMC solutions in different G/W mixtures were characterized using the DoS rheometry protocols. The radius evolution data for the NaCMC solutions with $M_w$ = 700 kDa display a relatively short apparent viscoelastic response, reminiscent of the datasets presented earlier for solutions of NaCMC of a lower $M_w$ = 250 kDa and polystyrene sulfonate solutions. In the semi-dilute regime, the measured values of extensional relaxation time and terminal, extensional viscosity appear to show a matched exponent for capturing the NaCMC


https://doi.org/10.1021/acs.macromol.2c00170
Macromolecules 2022, 55, 8117−8132

concentration-dependent variation for all glycerol concentrations. Finally, the polymer contribution to the Trouton ratio values for all glycerol systems calculated using the equation $Tr_P^{\infty} = (\eta_E^{\infty} - 3\eta_S)/(\eta_0 - \eta_S)$ fall within the same range of $Tr_P^{\infty} = 20-40$.

We infer that adding a solvent such as glycerol increases the shear viscosity, extensional viscosity, and extensional relaxation time of formulations, and thus, it functions as a thickener. However, the overall increase observed in absolute viscosity values of formulations containing polyelectrolytes need not be directly proportional to the increase in solvent viscosity. The influence of the dielectric constant on electrostatic interactions and the overall chain conformation varies and depends upon the polymer and solvent choices. Changes in polymer−solvent interactions due to variation in EV interactions, hydrogen bonding, and so forth, influence the manifested shear and extensional rheology response. We find that the concentration-dependent variation in specific viscosity, extensional viscosity, and extensional relaxation time cannot be simply modeled by accounting for the change in solvent viscosity and dielectric constant. Lastly, we observe that the extensional rheological response of cellulose gum solutions is less sensitive to solvent properties (glycerol fraction) and salt concentration than the shear rheological response, as the extensional rheological response is governed by dynamics of chains that undergo additional hydrodynamic stretch over and above the electrostatics-induced stretching that dictates the shear rheological response. As glycerol is a common additive in both food and cosmetic formulations, we envision that the results included in this study would provide industrial scientists a -deeper understanding of its influence on flow behavior and processability of multicomponent formulations, especially containing polyelectrolytes at a concentration below the tripling transition concentration.

## AUTHOR INFORMATION


### Corresponding Author

**Vivek Sharma** − *Department of Chemical Engineering, University of Illinois at Chicago, Chicago, Illinois 60607, United States;* orcid.org/0000-0003-1152-1285; Email: viveks@uic.edu

### Authors

**Leidy Nallely Jimenez** − *Department of Chemical Engineering, University of Illinois at Chicago, Chicago, Illinois 60607, United States*

**Carina D. V. Martínez Narváez** − *Department of Chemical Engineering, University of Illinois at Chicago, Chicago, Illinois 60607, United States;* orcid.org/0000-0002-2356-7208

Complete contact information is available at: https://pubs.acs.org/10.1021/acs.macromol.2c00170


### Notes

The authors declare no competing financial interest.

## ACKNOWLEDGMENTS

The authors would like to acknowledge funding support by the Motif Foodworks and PPG Industries, and L.N.J. and C.D. V. M. N,. acknowledge Teaching Assistantships in the Department of Chemistry and the Department of Chemical Engineering at UIC. We acknowledge discussions with current and former students at the ODES-lab at UIC, especially Nadia Nikolova, Lena Hassan, and Jelena Dinic.

## REFERENCES


(1) Dumitriu, S. *Polysaccharides: Structural Diversity and Functional Versality*, 2nd ed.; Marcel Dekker: New York, 2005.

(2) Kamide, K. *Cellulose and Cellulose Derivatives: Molecular Characterization and its Applications*; Elsevier: Amsterdam, 2005.

(3) Lapasin, R.; Pricl, S. *Rheology of Industrial Polysaccharides: Theory and Applications*; Chapman & Hall: London, 1995.

(4) Clasen, C.; Kulicke, W. M. Determination of viscoelastic and rheo-optical material functions of water-soluble cellulose derivatives. *Prog. Polym. Sci.* **2001**, *26*, 1839−1919.

(5) Lopez, C. G.; Rogers, S. E.; Colby, R. H.; Graham, P.; Cabral, J. T. Structure of sodium carboxymethyl cellulose aqueous solutions: A SANS and rheology study. *J. Polym. Sci., Part B: Polym. Phys.* **2015**, *53*, 492−501.

(6) Lopez, C. G.; Colby, R. H.; Graham, P.; Cabral, J. T. Viscosity and scaling of semiflexible polyelectrolyte NaCMC in aqueous salt solutions. *Macromolecules* **2017**, *50*, 332−338.

(7) Lopez, C. G.; Colby, R. H.; Cabral, J. T. Electrostatic and hydrophobic interactions in NaCMC aqueous solutions: Effect of degree of substitution. *Macromolecules* **2018**, *51*, 3165−3175.

(8) Wyatt, N. B.; Liberatore, M. W. Rheology and viscosity scaling of the polyelectrolyte xanthan gum. *J. Appl. Polym. Sci.* **2009**, *114*, 4076−4084.

(9) Zirnsak, M. A.; Boger, D. V.; Tirtaatmadja, V. Steady shear and dynamic rheological properties of xanthan gum solutions in viscous solvents. *J. Rheol.* **1999**, *43*, 627−650.

(10) Muthukumar, M. 50th anniversary perspective: A perspective on polyelectrolyte solutions. *Macromolecules* **2017**, *50*, 9528−9560.

(11) Dobrynin, A. V.; Rubinstein, M. Theory of polyelectrolytes in solutions and at surfaces. *Prog. Polym. Sci.* **2005**, *30*, 1049−1118.

(12) Holm, C.; Joanny, J.; Kremer, K.; Netz, R.; Reineker, P.; Seidel, C.; Vilgis, T. A.; Winkler, R. Polyelectrolyte theory. *Polyelectrolytes with Defined Molecular Architecture II*; Springer, 2004; pp 67−111.

(13) Wong, G. C. L.; Pollack, L. Electrostatics of strongly charged biological polymers: ion-mediated interactions and self-organization in nucleic acids and proteins. *Annu. Rev. Phys. Chem.* **2010**, *61*, 171−189.

(14) Muthukumar, M. Polyelectrolyte dynamics. *Adv. Chem. Phys.* **2005**, *131*, 1−60.

(15) Dobrynin, A. V. Solutions of charged polymers. *Polymer Science: A Comprehensive Reference* **2012**, *1*, 81−132.

(16) Barrat, J.-L.; Joanny, F. Theory of polyelectrolyte solutions. *Adv. Chem. Phys.* **1996**, *94*, 1.

(17) Dobrynin, A. V.; Colby, R. H.; Rubinstein, M. Scaling theory of polyelectrolyte solutions. *Macromolecules* **1995**, *28*, 1859−1871.

(18) Jimenez, L. N.; Dinic, J.; Parsi, N.; Sharma, V. Extensional relaxation time, pinch-off dynamics and printability of semi-dilute polyelectrolyte solutions. *Macromolecules* **2018**, *51*, 5191−5208.

(19) Jimenez, L. N.; Martínez Narváez, C. D. V.; Sharma, V. Capillary breakup and extensional rheology response of food thickener cellulose gum (NaCMC) in salt-free and excess salt solutions. *Phys. Fluids* **2020**, *32*, 012113.

(20) Staudinger, H.; Urech, E. Über hochpolymere Verbindungen. 31. Mitteilung. Über die Poly-acrylsäure und Poly-acrylsäure-ester. *Helv. Chim. Acta* **1929**, *12*, 1107−1133.

(21) Markovitz, H.; Kimball, G. E. The effect of salts on the viscosity of solutions of polyacrylic acid. *J. Colloid Sci.* **1950**, *5*, 115−139.

(22) Boris, D. C.; Colby, R. H. Rheology of sulfonated polystyrene solutions. *Macromolecules* **1998**, *31*, 5746−5755.

(23) Colby, R. H. Structure and linear viscoelasticity of flexible polymer solutions: comparison of polyelectrolyte and neutral polymer solutions. *Rheol. Acta* **2010**, *49*, 425−442.

(24) Dou, S.; Colby, R. H. Solution rheology of a strongly charged polyelectrolyte in good solvent. *Macromolecules* **2008**, *41*, 6505−6510.

(25) Sayko, R.; Jacobs, M.; Dobrynin, A. V. Quantifying Properties of Polysaccharide Solutions. *ACS Polymers Au* **2021**, *1*, 196−205.

(26) Dobrynin, A. V.; Jacobs, M.; Sayko, R. Scaling of polymer solutions as a quantitative tool. *Macromolecules* **2021**, *54*, 2288−2295.
(27) Jacobs, M.; Lopez, C. G.; Dobrynin, A. V. Quantifying the Effect of Multivalent Ions in Polyelectrolyte Solutions. *Macromolecules* **2021**, *54*, 9577−9586.
(28) Behra, J. S.; Mattsson, J.; Cayre, O. J.; Robles, E. S.; Tang, H.; Hunter, T. N. Characterization of sodium carboxymethyl cellulose aqueous solutions to support complex product formulation: A rheology and light scattering study. *ACS Appl. Polym. Mater.* **2019**, *1*, 344−358.
(29) Larson, R. G. The rheology of dilute solutions of flexible polymers: Progress and problems. *J. Rheol.* **2005**, *49*, 1−70.
(30) Nguyen, T. Q.; Kausch, H. H. *Flexible Polymer Chains in Elongational Flow: Theory and Experiment*; Springer-Verlag: Berlin, 1999.
(31) Sridhar, T. An overview of the project M1. *J. Non-Newtonian Fluid Mech.* **1990**, *35*, 85−92.
(32) James, D. F.; Walters, K. A critical appraisal of available methods for the measurement of extensional properties of mobile systems. In *Techniques of Rheological Measurement*; Collyer, A. A., Ed.; Elsevier: New York, 1994; pp 33−53.
(33) Sharma, V.; Haward, S. J.; Serdy, J.; Keshavarz, B.; Soderlund, A.; Threlfall-Holmes, P.; McKinley, G. H. The rheology of aqueous solutions of Ethyl Hydroxy-Ethyl Cellulose (EHEC) and its hydrophobically modified analogue (hmEHEC): Extensional flow response in capillary break-up, jetting (ROJER) and in a cross-slot extensional rheometer. *Soft Matter* **2015**, *11*, 3251−3270.
(34) McKinley, G. H. Visco-elasto-capillary thinning and break-up of complex fluids. *Rheol. Rev.* **2005**, 1−48.
(35) Rodd, L. E.; Scott, T. P.; Cooper-White, J. J.; McKinley, G. H. Capillary break-up rheometry of low-viscosity elastic fluids. *Appl. Rheol.* **2005**, *15*, 12−27.
(36) Petrie, C. J. S. One hundred years of extensional flow. *J. Non-Newtonian Fluid Mech.* **2006**, *137*, 1−14.
(37) Dinic, J.; Sharma, V. Power laws dominate shear and extensional rheology response and capillarity-driven pinching dynamics of entangled hydrodyethyl cellulose (HEC) solutions. *Macromolecules* **2020**, *53*, 3424−3437.
(38) De Dier, R.; Mathues, W.; Clasen, C. Extensional flow and relaxation of semi-dilute solutions of schizophyllan. *Macromol. Mater. Eng.* **2013**, *298*, 944−953.
(39) Vadodaria, S. S.; English, R. J. Extensional rheometry of cellulose ether solutions: flow instability. *Cellulose* **2016**, *23*, 339−355.
(40) Haward, S. J.; Sharma, V.; Butts, C. P.; McKinley, G. H.; Rahatekar, S. S. Shear and extensional rheology of cellulose/ionic liquid solutions. *Biomacromolecules* **2012**, *13*, 1688−1699.
(41) Khagram, M.; Gupta, R. K.; Sridhar, T. Extensional flow of xanthan gum solutions. *J. Rheol.* **1985**, *29*, 191−207.
(42) Carrington, S.; Odell, J.; Fisher, L.; Mitchell, J.; Hartley, L. Polyelectrolyte behaviour of dilute xanthan solutions: Salt effects on extensional rheology. *Polymer* **1996**, *37*, 2871−2875.
(43) Choi, H.; Mitchell, J. R.; Gaddipati, S. R.; Hill, S. E.; Wolf, B. Shear rheology and filament stretching behaviour of xanthan gum and carboxymethyl cellulose solution in presence of saliva. *Food Hydrocolloids* **2014**, *40*, 71−75.
(44) Gilbert, L.; Loisel, V.; Savary, G.; Grisel, M.; Picard, C. Stretching properties of xanthan, carob, modified guar and celluloses in cosmetic emulsions. *Carbohydr. Polym.* **2013**, *93*, 644−650.
(45) González, J. M.; Müller, A. J.; Torres, M. F.; Sáez, A. E. The role of shear and elongation in the flow of solutions of semi-flexible polymers through porous media. *Rheol. Acta* **2005**, *44*, 396−405.
(46) Martín-Alfonso, J. E.; Cuadri, A. A.; Berta, M.; Stading, M. Relation between concentration and shear-extensional rheology properties of xanthan and guar gum solutions. *Carbohydr. Polym.* **2018**, *181*, 63−70.
(47) Miles, M. J.; Tanaka, K.; Keller, A. The behavior of polyelectrolytes in elongational flow; the determination of conformational relaxation times (with an Appendix of an anomalous adsorption effect. *Polymer* **1983**, *24*, 1081−1088.
(48) Narh, K. A.; Odell, J. A.; Keller, A. Temperature dependence of the conformational relaxation time of polymer molecules in elongational flow; invariance of the molecular weight exponent. *J. Polym. Sci., Part B: Polym. Phys.* **1992**, *30*, 335−340.
(49) Narh, K. A.; Keller, A. The effect of counterions on the chain conformation of polyelectrolytes, as assessed by extensibility in elongational flow: The influence of multiple valency. *J. Polym. Sci., Part B: Polym. Phys.* **1994**, *32*, 1697−1706.
(50) Dunlap, P. N.; Leal, L. G. The charged dumbbell model for dilute polyelectrolyte solutions in strong flows. *Rheol. Acta* **1984**, *23*, 238−249.
(51) Dunlap, P. N.; Wang, C. H.; Leal, L. G. An experimental study of dilute polyelectrolyte solutions in strong flows. *J. Polym. Sci., Part B: Polym. Phys.* **1987**, *25*, 2211−2238.
(52) Borisov, O. V.; Darinskii, A. A.; Zhulina, E. B. Stretching of polyelectrolyte coils and globules in an elongational flow. *Macromolecules* **1995**, *28*, 7180−7187.
(53) Darinskii, A. A.; Borisov, O. V. Polyelectrolyte molecule in an elongational flow. *Europhys. Lett.* **1995**, *29*, 365−370.
(54) Funatsu, Y.; Fukao, K.; Miyamoto, Y. Elongational flow study of poly(styrene sulfonate) in dilute solution. *Polymer* **1997**, *38*, 2857−2860.
(55) Liu, S.; Ashok, B.; Muthukumar, M. Brownian dynamics simulations of bead-rod-chain in simple shear flow and elongational flow. *Polymer* **2004**, *45*, 1383−1389.
(56) Stelter, M.; Brenn, G.; Yarin, A. L.; Singh, R. P.; Durst, F. Validation and application of a novel elongational device for polymer solutions. *J. Rheol.* **2000**, *44*, 595−616.
(57) Andrews, N. C.; McHugh, A. J.; Schieber, J. D. Polyelectrolytes in shear and extensional flows: Conformation and rheology. *J. Polym. Sci., Part B: Polym. Phys.* **1998**, *36*, 1401−1417.
(58) Jiang, L.; Chen, S. B. Electroviscous effect on the rheology of a dilute solution of flexible polyelectrolytes in extensional flow. *J. Non-Newtonian Fluid Mech.* **2001**, *96*, 445−458.
(59) Pamies, R.; Cifre, J. G. H.; De La Torre, J. G. Brownian dynamics simulation of polyelectrolyte dilute solutions: Relaxation time and elongational flow. *J. Polym. Sci., Part B: Polym. Phys.* **2007**, *45*, 714−722.
(60) Sasaki, N.; Ashitaka, H.; Ohtomo, K.; Fukui, A. Hydrodynamic properties of DNA and DNA-lipid complex in an elongational flow field. *Int. J. Biol. Macromol.* **2007**, *40*, 327−335.
(61) Stoltz, C.; de Pablo, J. J.; Graham, M. D. Concentration dependence of shear and extensional rheology of polymer solutions: Brownian dynamics simulations. *J. Rheol.* **2006**, *50*, 137−167.
(62) Entov, V. M.; Hinch, E. J. Effect of a spectrum of relaxation times on the capillary thinning of a filament of elastic liquid. *J. Non-Newtonian Fluid Mech.* **1997**, *72*, 31−53.
(63) Anna, S. L.; McKinley, G. H. Elasto-capillary thinning and breakup of model elastic liquids. *J. Rheol.* **2001**, *45*, 115−138.
(64) Dinic, J.; Martínez Narváez, C. D. V.; Sharma, V. Rheology of Unentangled Polymer Solutions Depends on Three Macromolecular Properties: Flexibility, Extensibility, and Segmental Dissymmetry. In *Macromolecular Engineering*; Hadjichristidis, N., Gnanou, Y., Matyjaszewski, K., Muthukumar, M., Eds.; Wiley Online, 2022; pp 1−36. DOI: 10.1002/9783527815562.mme0067
(65) Dinic, J.; Sharma, V. Macromolecular relaxation, strain, and extensibility determine elastocapillary thinning and extensional viscosity of polymer solutions. *Proc. Natl. Acad. Sci. U.S.A.* **2019**, *116*, 8766−8774.
(66) Dinic, J.; Biagioli, M.; Sharma, V. Pinch-off dynamics and extensional relaxation times of intrinsically semi-dilute polymer solutions characterized by dripping-onto-substrate rheometry. *J. Polym. Sci., Part B: Polym. Phys.* **2017**, *55*, 1692−1704.
(67) Dinic, J.; Zhang, Y.; Jimenez, L. N.; Sharma, V. Extensional relaxation times of dilute, aqueous polymer solutions. *ACS Macro Lett.* **2015**, *4*, 804−808.
(68) Dinic, J.; Jimenez, L. N.; Sharma, V. Pinch-off dynamics and dripping-onto-substrate (DoS) rheometry of complex fluids. *Lab Chip* **2017**, *17*, 460−473.

(69) Dinic, J.; Sharma, V. Flexibility, extensibility, and ratio of Kuhn length to packing length govern the pinching gynamics, coil-stretch transition, and rheology of polymer solutions. *Macromolecules* **2020**, *53*, 4821−4835.
(70) Martínez Narváez, C. D. V.; Dinic, J.; Lu, X.; Wang, C.; Rock, R.; Sun, H.; Sharma, V. Rheology and pinching dynamics of associative polysaccharide solutions. *Macromolecules* **2021**, *54*, 6372−6388.
(71) Paul, S. H.; Adeniyi, O. D.; Olutoye, M. A. Production and Characterization of Soymilk Using Locally Prepared Date Paste (Phoenix Dactylifera), White Sugar and Glycerol as Sweeteners. *Current Trends in Biomedica l Engineering & Biosciences* **2017**, *7*, 555709.
(72) Habchi, W.; Matta, C.; Joly-Pottuz, L.; De Barros, M.; Martin, J.; Vergne, P. Full film, boundary lubrication and tribochemistry in steel circular contacts lubricated with glycerol. *Tribol. Lett.* **2011**, *42*, 351.
(73) Stout, E. I.; McKessor, A. Glycerin-based hydrogel for infection control. *Adv. Wound Care* **2012**, *1*, 48−51.
(74) Gross, F. C.; Jones, J. H. Determination of Glycerol in Cosmetics by GLC. I. Development of the Method. *J. Assoc. Off. Anal. Chem.* **1967**, *50*, 1287−1291.
(75) Tan, H.; Abdul Aziz, A. A.; Aroua, M. Glycerol production and its applications as a raw material: A review. *Renew. Sustain. Energy Rev.* **2013**, *27*, 118−127.
(76) Behr, A.; Eilting, J.; Irawadi, K.; Leschinski, J.; Lindner, F. Improved utilisation of renewable resources: New important derivatives of glycerol. *Green Chem.* **2008**, *10*, 13−30.
(77) Pagliaro, M.; Ciriminna, R.; Kimura, H.; Rossi, M.; Della Pina, C. From glycerol to value-added products. *Angew. Chem., Int. Ed.* **2007**, *46*, 4434−4440.
(78) Pagliaro, M. *Glycerol: The Renewable Platform Chemical*; Elsevier, 2017.
(79) Wüstenberg, T. *Cellulose and Cellulose Derivatives in the Food Industry: Fundamentals and Applications*; John Wiley & Sons, 2014.
(80) Guo, J.-H.; Skinner, G. W.; Harcum, W. W.; Barnum, P. E. Pharmaceutical applications of naturally occurring water-soluble polymers. *Pharm. Sci. Technol. Today* **1998**, *1*, 254−261.
(81) Jones, D. S.; Woolfson, A. D.; Brown, A. F. Textural, viscoelastic and mucoadhesive properties of pharmaceutical gels composed of cellulose polymers. *Int. J. Pharm.* **1997**, *151*, 223−233.
(82) Gordon, R.; Orias, R.; Willenbacher, N. Effect of carboxymethyl cellulose on the flow behavior of lithium-ion battery anode slurries and the electrical as well as mechanical properties of corresponding dry layers. *J. Mater. Sci.* **2020**, *55*, 15867−15881.
(83) Lopez, C. G.; Richtering, W. Influence of divalent counterions on the solution rheology and supramolecular aggregation of carboxymethyl cellulose. *Cellulose* **2019**, *26*, 1517−1534.
(84) Arancibia, C.; Bayarri, S.; Costell, E. Comparing carboxymethyl cellulose and starch as thickeners in oil/water emulsions. Implications on rheological and structural properties. *Food Biophys.* **2013**, *8*, 122−136.
(85) Cancela, M.; Álvarez, E.; Maceiras, R. Effects of temperature and concentration on carboxymethylcellulose with sucrose rheology. *J. Food Eng.* **2005**, *71*, 419−424.
(86) Ghannam, M. T.; Esmail, M. N. Rheological properties of carboxymethyl cellulose. *J. Appl. Polym. Sci.* **1997**, *64*, 289−301.
(87) Yuliarti, O.; Mei, K. H.; Kam Xue Ting, Z. K. X.; Yi, K. Y. Influence of combination carboxymethylcellulose and pectin on the stability of acidified milk drinks. *Food Hydrocolloids* **2019**, *89*, 216−223.
(88) Wunderlich, T.; Stelter, M.; Tripathy, T.; Nayak, B.; Brenn, G.; Yarin, A.; Singh, R.; Brunn, P.; Durst, F. Shear and extensional rheological investigations in solutions of grafted and ungrafted polysaccharides. *J. Appl. Polym. Sci.* **2000**, *77*, 3200−3209.
(89) Yang, X. H.; Zhu, W. L. Viscosity properties of sodium carboxymethylcellulose solutions. *Cellulose* **2007**, *14*, 409−417.
(90) Dapía, S.; Tovar, C. A.; Santos, V.; Parajó, J. C. Rheological behaviour of carboxymethylcellulose manufactured from TCF-bleached milox pulps. *Food Hydrocolloids* **2005**, *19*, 313−320.
(91) deButts, E. H.; Hudy, J. A.; Elliott, J. H. Rheology of sodium carboxymethylcellulose solutions. *Ind. Eng. Chem.* **1957**, *49*, 94−98.
(92) Elliot, J. H.; Ganz, A. J. Some rheological properties of sodium carboxymethylcellulose solutions and gels. *Rheol. Acta* **1974**, *13*, 670−674.
(93) Horinaka, J.-i.; Chen, K.; Takigawa, T. Entanglement properties of carboxymethyl cellulose and related polysaccharides. *Rheol. Acta* **2018**, *57*, 51−56.
(94) Komorowska, P.; Różańska, S.; Różański, J. Effect of the degree of substitution on the rheology of sodium carboxymethylcellulose solutions in propylene glycol/water mixtures. *Cellulose* **2017**, *24*, 4151−4162.
(95) Lopez, C. G. Entanglement of semiflexible polyelectrolytes: Crossover concentrations and entanglement density of sodium carboxymethyl cellulose. *J. Rheol.* **2020**, *64*, 191−204.
(96) Lopez, C. G.; Richtering, W. Oscillatory rheology of carboxymethyl cellulose gels: Influence of concentration and pH. *Carbohydr. Polym.* **2021**, *267*, 118117.
(97) Różańska, S.; Verbeke, K.; Różański, J.; Clasen, C.; Wagner, P. Capillary breakup extensional rheometry of sodium carboxymethyl-cellulose solutions in water and propylene glycol/water mixtures. *J. Polym. Sci., Part B: Polym. Phys.* **2019**, *57*, 1537−1547.
(98) Lopez, C. G. Entanglement properties of polyelectrolytes in salt-free and excess-salt solutions. *ACS Macro Lett.* **2019**, *8*, 979−983.
(99) Martínez Narváez, C. D. V.; Mazur, T.; Sharma, V. Dynamics and extensional rheology of polymer-surfactant association complexes. *Soft Matter* **2021**, *17*, 6116−6126.
(100) Jimenez, L. N.; Martínez Narváez, C. D. V.; Xu, C.; Bacchi, S.; Sharma, V. The rheologically-complex fluid beauty of nail lacquer formulations. *Soft Matter* **2021**, *17*, 5197.
(101) Jimenez, L. N.; Martínez Narváez, C. D. V.; Xu, C.; Bacchi, S.; Sharma, V. Rheological properties influence tackiness, application and performance of nail polish/lacquer formulations in *Surface Science and Adhesion in Cosmetics* Mittal, K. L.; Bui, H. S., Eds. 2021109−150
(102) Merchiers, J.; Martínez Narváez, C. D. V.; Slykas, C.; Reddy, N. K.; Sharma, V. Evaporation and rheology chart the processability map for centrifugal force spinning. *Macromolecules* **2021**, *54*, 11061−11073.
(103) Hsiao, K. W.; Dinic, J.; Ren, Y.; Sharma, V.; Schroeder, C. M. Passive non-linear microrheology for determining extensional viscosity. *Phys. Fluids* **2017**, *29*, 121603.
(104) Walter, A. V.; Jimenez, L. N.; Dinic, J.; Sharma, V.; Erk, K. A. Effect of salt valency and concentration on shear and extensional rheology of aqueous polyelectrolyte solutions for enhanced oil recovery. *Rheol. Acta* **2019**, *58*, 145−157.
(105) Merchiers, J.; Slykas, C. L.; Martínez Narváez, C. D.; Buntinx, M.; Deferme, W.; Peeters, R.; Reddy, N. K.; Sharma, V. Fiber Engineering Trifecta of Spinnability, Morphology, and Properties: Centrifugally Spun versus Electrospun Fibers. *ACS Appl. Polym. Mater.* **2022**, *4*, 2022−2035.
(106) Marshall, K. A.; Liedtke, A. M.; Todt, A. H.; Walker, T. W. Extensional rheometry with a handheld mobile device. *Exp. Fluid* **2017**, *58*, 69.
(107) Marshall, K. A.; Walker, T. W. Investigating the dynamics of droplet breakup in a microfluidic cross-slot device for characterizing the extensional properties of weakly-viscoelastic fluids. *Rheol. Acta* **2019**, *58*, 573−590.
(108) Pack, M. Y.; Yang, A.; Perazzo, A.; Qin, B.; Stone, H. A. Role of extensional rheology on droplet bouncing. *Phys. Rev. Fluids* **2019**, *4*, 123603.
(109) Suteria, N. S.; Gupta, S.; Potineni, R.; Baier, S. K.; Vanapalli, S. A. eCapillary: a disposable microfluidic extensional viscometer for weakly elastic polymeric fluids. *Rheol. Acta* **2019**, *58*, 403−417.
(110) Xu, M.; Li, X.; Riseman, A.; Frostad, J. M. Quantifying the effect of extensional rheology on the retention of agricultural sprays. *Phys. Fluids* **2021**, *33*, 032107.


https://doi.org/10.1021/acs.macromol.2c00170
*Macromolecules* 2022, 55, 8117−8132

(111) Su, Y.; Palacios, B.; Zenit, R. Coiling of a viscoelastic fluid filament. *Phys. Rev. Fluids* **2021**, *6*, 033303.
(112) Rosello, M.; Sur, S.; Barbet, B.; Rothstein, J. P. Dripping-onto-substrate capillary breakup extensional rheometry of low-viscosity printing inks. *J. Non-Newtonian Fluid Mech.* **2019**, *266*, 160−170.
(113) Murdoch, T. J.; Pashkovski, E.; Patterson, R.; Carpick, R. W.; Lee, D. Sticky but Slick: Reducing Friction Using Associative and Nonassociative Polymer Lubricant Additives. *ACS Appl. Polym. Mater.* **2020**, *2*, 4062−4070.
(114) Wu, S.; Mohammadigoushki, H. Linear versus branched: flow of a wormlike micellar fluid past a falling sphere. *Soft Matter* **2021**, *17*, 4395−4406.
(115) Franco-Gómez, A.; Onuki, H.; Yokoyama, Y.; Nagatsu, Y.; Tagawa, Y. Effect of liquid elasticity on the behaviour of high-speed focused jets. *Exp. Fluid* **2021**, *62*, 41.
(116) Jafari Nodoushan, E.; Lee, Y. J.; Lee, G.-H.; Kim, N. Quasi-static secondary flow regions formed by microfluidic contraction flows of wormlike micellar solutions. *Phys. Fluids* **2021**, *33*, 093112.
(117) Brückner, A.; Badroos, J. M.; Learsch, R. W.; Yousefelahiyeh, M.; Kitchen, S. A.; Parker, J. Evolutionary assembly of cooperating cell types in an animal chemical defense system. *Cell* **2021**, *184*, 6138−6156.e28.
(118) Fuoss, R. M. Polyelectrolytes. *Discuss. Faraday Soc.* **1951**, *11*, 125−134.
(119) Fuoss, R. M.; Strauss, U. P. Polyelectrolytes. II. Poly-4-vinylpyridonium chloride and poly-4-vinyl-N-n-butylpyridonium bromide. *J. Polym. Sci.* **1948**, *3*, 246−263.
(120) Oelschlaeger, C.; Cota Pinto Coelho, M. C. P.; Willenbacher, N. Chain Flexibility and Dynamics of Polysaccharide Hyaluronan in Entangled Solutions: A High Frequency Rheology and Diffusing Wave Spectroscopy Study. *Biomacromolecules* **2013**, *14*, 3689−3696.
(121) Üzüm, C.; Christau, S.; von Klitzing, R. Structuring of Polyelectrolyte (NaPSS) Solutions in Bulk and under Confinement as a Function of Concentration and Molecular Weight. *Macromolecules* **2011**, *44*, 7782−7791.
(122) Uematsu, Y.; Araki, T. Electro-osmotic flow of semi-dilute polyelectrolyte solutions. *J. Chem. Phys.* **2013**, *139*, 094901.
(123) Cohen, J.; Priel, Z. Intrinsic viscosity of polyelectrolyte solutions. *Polym. Commun.* **1989**, *30*, 223−224.
(124) Eisenberg, H.; Pouyet, J. Viscosities of dilute aqueous solutions of a partially quaternized poly-4-vinyl pyridine at low gradients of flow. *J. Polym. Sci.* **1954**, *13*, 85−91.
(125) Roure, I.; Rinaudo, M.; Milas, M.; Frollini, E. Viscometric behaviour of polyelectrolytes in the presence of low salt concentration. *Polymer* **1998**, *39*, 5441−5445.
(126) Netz, R. R.; Andelman, D. Neutral and charged polymers at interfaces. *Phys. Rep.* **2003**, *380*, 1−95.
(127) Muthukumar, M. Theory of viscoelastic properties of polyelectrolyte solutions. *Polymer* **2001**, *42*, 5921−5923.
(128) Krause, W. E.; Tan, J. S.; Colby, R. H. Semidilute solution rheology of polyelectrolytes with no added salt. *J. Polym. Sci., Part B: Polym. Phys.* **1999**, *37*, 3429−3437.
(129) Witten, T. A.; Pincus, P. Structure and viscosity of interpenetrating polyelectrolyte chains. *Europhys. Lett.* **1987**, *3*, 315.
(130) Prini, R. F.; Lagos, A. E. Tracer diffusion, electrical conductivity, and viscosity of aqueous solutions of polystyrenesulfonates. *J. Polym. Sci., Part A: Polym. Chem.* **1964**, *2*, 2917−2928.
(131) Cohen, J.; Priel, Z. Viscosity of dilute polyelectrolyte solutions: temperature dependence. *J. Chem. Phys.* **1990**, *93*, 9062−9068.
(132) Oostwal, M. G.; Blees, M. H.; De Bleijser, J.; Leyte, J. C. Chain self-diffusion in aqueous salt-free solutions of sodium poly (styrenesulfonate). *Macromolecules* **1993**, *26*, 7300−7308.
(133) Chen, S. P.; Archer, L. A. Relaxation dynamics of salt-free polyelectrolyte solutions using flow birefringence and rheometry. *J. Polym. Sci., Part B: Polym. Phys.* **1999**, *37*, 825−835.
(134) Muthukumar, M. Dynamics of polyelectrolyte solutions. *J. Chem. Phys.* **1997**, *107*, 2619−2635.
(135) Dou, S.; Colby, R. H. Charge density effects in salt-free polyelectrolyte solution rheology. *J. Polym. Sci., Part B: Polym. Phys.* **2006**, *44*, 2001−2013.
(136) Shankar, R.; Klossner, R. R.; Weaver, J. T.; Koga, T.; van Zanten, J. H.; Krause, W. E.; Colina, C. M.; Tanaka, F.; Spontak, R. J. Competitive hydrogen-bonding in polymer solutions with mixed solvents. *Soft Matter* **2009**, *5*, 304−307.
(137) Rubinstein, M.; Colby, R. H. *Polymer Physics*; Oxford Univ. Press: New York, 2003.
(138) Han, A.; Colby, R. H. Rheology of entangled polyelectrolyte solutions. *Macromolecules* **2021**, *54*, 1375−1387.
(139) Fardin, M.-A.; Hautefeuille, M.; Sharma, V. Spreading, pinching, and coalescence: the Ohnesorge units. *Soft Matter* **2022**, *18*, 3291−3303.
(140) McKinley, G. H.; Tripathi, A. How to extract the Newtonian viscosity from capillary breakup measurements in a filament rheometer. *J. Rheol.* **2000**, *44*, 653−670.
(141) Dinic, J.; Sharma, V. Computational analysis of self-similar capillary-driven thinning and pinch-off dynamics during dripping using the volume-of-fluid method. *Phys. Fluids* **2019**, *31*, 021211.
(142) Deblais, A.; Herrada, M. A.; Hauner, I.; Velikov, K. P.; van Roon, T.; Kellay, H.; Eggers, J.; Bonn, D. Viscous Effects on Inertial Drop Formation. *Phys. Rev. Lett.* **2018**, *121*, 254501.
(143) Zhou, J.; Doi, M. Dynamics of viscoelastic filaments based on Onsager principle. *Phys. Rev. Fluids* **2018**, *3*, 084004.
(144) Clasen, C.; Plog, J. P.; Kulicke, W. M.; Owens, M.; Macosko, C.; Scriven, L. E.; Verani, M.; McKinley, G. H. How dilute are dilute solutions in extensional flows? *J. Rheol.* **2006**, *50*, 849−881.
(145) Ardekani, A.; Sharma, V.; McKINLEY, G. H. Dynamics of bead formation, filament thinning and breakup of weakly viscoelastic jets. *J. Fluid Mech.* **2010**, *665*, 46−56.
(146) Wagner, C.; Bourouiba, L.; McKinley, G. H. An analytic solution for capillary thinning and breakup of FENE-P fluids. *J. Non-Newtonian Fluid Mech.* **2015**, *218*, 53−61.
(147) Eggers, J.; Herrada, M. A.; Snoeijer, J. H. Self-similar breakup of polymeric threads as described by the Oldroyd-B model. *J. Fluid Mech.* **2020**, *887*.A19 DOI: 10.1017/jfm.2020.18
(148) Deblais, A.; Herrada, M. A.; Eggers, J.; Bonn, D. Self-similarity in the breakup of very dilute viscoelastic solutions. *J. Fluid Mech.* **2020**, *904*.R2 DOI: 10.1017/jfm.2020.765
(149) Bhat, P. P.; Appathurai, S.; Harris, M. T.; Pasquali, M.; McKinley, G. H.; Basaran, O. A. Formation of beads-on-a-string structures during break-up of viscoelastic filaments. *Nat. Phys.* **2010**, *6*, 625−631.
(150) Yarin, A. L. *Free Liquid Jets and Films: Hydrodynamics and Rheology*; Longman Scientific & Technical, 1993.
(151) Bird, R. B.; Armstrong, R. C.; Hassager, O. *Dynamics of Polymeric Liquids*, 2nd ed.; John Wiley & Sons: New York, 1987; Vol. *1*.
(152) Prabhakar, R.; Sasmal, C.; Nguyen, D. A.; Sridhar, T.; Prakash, J. R. Effect of stretching-induced changes in hydrodynamic screening on coil-stretch hysteresis of unentangled polymer solutions. *Phys. Rev. Fluids* **2017**, *2*, 011301.
(153) Prabhakar, R.; Prakash, J. R.; Sridhar, T. Effect of configuration-dependent intramolecular hydrodynamic interaction on elastocapillary thinning and breakup of filaments of dilute polymer solutions. *J. Rheol.* **2006**, *50*, 925−947.
(154) Prabhakar, R.; Gadkari, S.; Gopesh, T.; Shaw, M. J. Influence of stretching induced self-concentration and self-dilution on coil-stretch hysteresis and capillary thinning of unentangled polymer solutions. *J. Rheol.* **2016**, *60*, 345−366.
(155) Prakash, J. R. Universal dynamics of dilute and semi-dilute solutions of flexible linear polymers. *Curr. Opin. Colloid Interface Sci.* **2019**, *43*, 63−79.
(156) Larson, R. G. *Constitutive Equations for Polymer Solutions and Melts*; Butterworth Publishers: Boston, 1988.
(157) Matsumiya, Y.; Watanabe, H. Non-Universal features in uniaxially extensional rheology of linear polymer melts and concentrated solutions: A review. *Prog. Polym. Sci.* **2020**, *112*, 101325.

(158) Desai, P. S.; Larson, R. G. Constitutive model that shows extension thickening for entangled solutions and extension thinning for melts. *J. Rheol.* **2014**, *58*, 255−279.





https://doi.org/10.1021/acs.macromol.2c00170
*Macromolecules* 2022, 55, 8117−8132